UNIVERSITY OF OKLAHOMA

GRADUATE COLLEGE

ASSESSMENT OF THE SEVERE WEATHER ENVIRONMENT IN NORTH AMERICA SIMULATED BY A GLOBAL CLIMATE MODEL

A THESIS

SUBMITTED TO THE GRADUATE FACULTY

in partial fulfillment of the requirements for the

Degree of

MASTER OF SCIENCE IN METEOROLOGY

By

PATRICK TIMOTHY MARSH
Norman, Oklahoma
2007

ASSESSMENT OF THE SEVERE WEATHER ENVIRONMENT IN NORTH AMERICA SIMULATED BY A GLOBAL CLIMATE MODEL: CURRENT AND FUTURE

A THESIS APPROVED FOR THE
SCHOOL OF METEOROLOGY

BY

_____
Harold E. Brooks, Chair

_____
David J. Karoly

_____
Kelvin K. Droegemeier

_____
Kevin Kloesel

©Copyright by PATRICK TIMOTHY MARSH 2007
All Rights Reserved.

Acknowledgements

First, and foremost, I would like to thank my wife Sarah for her continual love and support over the past 2+ years. Whether I was pulling all nighters, sleeping all day to catch up, or was just plain cranky because my computer had died yet again, she was always there for me. I would also like to thank my extended family for being supportive and understanding as I worked through many family trips and holidays.

I am indebted to my principal advisers Drs. Harold Brooks and David Karoly. They have encouraged and guided me along the way and have provided ample opportunity to expand my knowledge on this subject. I would also like to thank my other committee members Drs. Kelvin Droegemeier and Kevin Kloesel for being understanding about all the mix-ups and catastrophes that have occurred in the past 2 months.

There are many people at the University of Oklahoma who I owe a lot of thanks especially my friends, especially Kevin Goebbert, Chad Shafer, M.O.Nkey, and Dr. Mark Laufersweiler. Without our way-to-frequent gripe sessions, I would be an even crankier person today. I would also like to thank my office-mate Melissa Bukovsky for her gracious help in teaching me how to use NCL (and for listening to my numerous rants about what went wrong this time).

Finally, I would like to thank my mentor and friend Forrest Johns who passed away during the research for this thesis. Without his friendship and support for all those years, I know I would not be here now. This is dedicated to his memory and our friendship.

Table of Contents

List of Figures……vi
Abstract…….....viii
Chapter 1: Introduction……...1
Chapter 2: Description of the Models……....13
Section 2.1: Community Climate Systems Model 3 (CCSM3)……...…..13
Section 2.2: Reanalysis Data…….....16
Chapter 3: Methodology……....18
Section 3.1: Calculation of Atmospheric Variables……...18
Section 3.2: Analysis of CCSM3 Severe Weather Environment……..…..22
Chapter 4: Current Climate Simulation…….……....24
Section 4.1: Results from CCSM3 20th Century Simulation…….24
Section 4.2: Discussion……..39
Chapter 5: Future Climate Simulations…….41
Section 5.1: Results from CCSM3 SRES A2 21st Century Simulation…….42
Section 5.2: Discussion……..56
Chapter 6: Discussion……...…59
References……63

List of Figures

Figure 1.1: IPCC Future Temperature Projections……..……..…3

Figure 1.2: Effect of Increasing Mean and Variance on Temperature……..4

Figure 1.3.1: Fatalities Per Year Resulting From Severe Convective Weather……....5

Figure 1.3.2: Injuries Per Year Resulting From Severe Convective Weather……..….5

Figure 1.4: Costs Per Year Resulting From Severe Convective Weather……..…..…….6

Figure 1.5: Number of Days Per Year With Favorable Severe Parameters……..9

Figure 3.1: Mean Season CAPE Comparison Between Routines……21

Figure 4.1: Mean Seasonal Cycle of CAPE……..…26

Figure 4.2: Combined North American Frequency Distribution……..…29

Figure 4.3: Combined Central United States Frequency Distribution…….……30

Figure 4.4: Joint Distribution of Deep Layer Shear and CAPE…….…..32

Figure 4.5: Annual Number of Days with Favorable Severe Parameters……..…33

Figure 4.6: Annual Number of Days with Favorable Severe Parameters – Central…..…34

Figure 4.7: Monthly and Diurnal Cycle of Mean CAPE……..37

Figure 4.8: Interannual Variability of Mean CAPE…….…….38

Figure 5.1: Mean Seasonal Cycle of CAPE…….……44

Figure 5.2: Mean Season Cycle of Deep Layer Shear…….…….45

Figure 5.3: Combined North American Frequency Distribution…….…..…48

Figure 5.4: Combined Central United States Frequency Distribution…….…….49

Figure 5.5: Joint Distribution of Deep Layer Shear and CAPE…….……..50

Figure 5.6: Annual Number of Days with Favorable Severe Parameters…….……51

Figure 5.7: Annual Number of Days with Favorable Severe Parameters – Central…..…53

Figure 5.8: Monthly and Diurnal Cycle of Mean CAPE……..54

Figure 5.9: Interannual Variability of Mean CAPE…….…….55

Abstract

Global Climate Models (GCMs) are becoming increasingly important in the simulation of climate change associated with increases in greenhouse gas concentrations in the atmosphere. However, little, if anything, has been said about the erects of increased anthropogenic forcing on severe convective weather. Recent improvements in global climate model resolution and increased data storage capabilities have allowed for climate simulations or resolutions similar to those of the NCAR / NCEP global reanalysis to be archived at six hour intervals.

Brooks et al. (2003) demonstrated that probability of occurrence of significant severe convective weather increases with increasing Convective Available Potential Energy (CAPE) and 0 to 6 kilometer deep layer shear. Additionally, Brooks et al. (2003) went on to demonstrate that the NCAR / NCEP global reanalysis data can be used as a surrogate for observational fields of CAPE, deep layer shear, and their combination. The methodology used by Brooks et al. (2003) serves as the basis to examine changes in the severe convective weather environment in North America under global warming as simulated by the NCAR CCSM3 global climate model.

A comparison of the current CCSM3 severe convective weather environment to that of the global reanalysis data will be presented to illustrate the ability of the CCSM3 to simulate the current severe convective weather environment qualitatively. This will be followed by a preliminary examination of the severe weather environment at the end of the 21st century simulated by the CCSM3 under the A2 SRES emission scenario. The focus will be on comparing current CCSM3 model output and global reanalysis distributions of CAPE, deep layer shear, and their combination for the current severe

convective weather environment. This will be followed by an examination of the future severe convective weather environment simulated by the CCSM3 compared to the current environment as simulated by the CCSM3. This will be followed by a brief discussion of projected changes in the probability of occurrence of severe convective weather environments in North America.

Chapter 1: Introduction

People often colloquially define weather as what is currently happening while climate is defined as what is expected to happen. While this is overly simplistic, it strikes at the heart of what climate really is – the long term combination of short term weather conditions. Using the aforementioned definition, climate change can be explained as a change in what weather conditions are expected in a given region. However this definition provides more questions than answers, such as how long must the weather conditions at a given location be different before the climate is changed. There is not a simple answer to this question as the climate may change in various ways over various time scales.

Typically, climate change is defined as any discernable change in any aspect of the present climate, such as temperature, moisture content, or precipitation, persisting on time scales of at least a decade (AMS, 2000). These changes can occur from a variety of means including, but not limited to, changes in anthropogenic forcing (greenhouse gases and aerosols in the atmosphere) and solar activity. Presently a scientific (and public) debate is raging as to whether increasing greenhouse gases will result in an increase in anthropogenic forcing and in turn lead to global warming – a form of climate change in which the mean surface temperature of earth increases. Topics currently debated range from whether an increase in greenhouse gasses is leading / will lead to global warming to what impacts can be expected due to global warming induced by an increase in greenhouse gasses (hereafter referred to as simply global warming). It is beyond the scope of this study

to jump into the middle of this debate and thus the author will defer to the findings of the Intergovernmental Panel on Climate Change (IPCC).

Figure 1.1 shows the projected increase in temperature through 2100 from a suite of ensembles used by the IPCC in their Fourth Assessment Report (AR4). It is readily apparent from figure 1.1 that all models in all emission scenarios show an increase in mean temperature by the end of the 21st century. Figure 1.2 demonstrates the effect of increasing the variance as well as the mean temperature. An increase in the mean temperature results in more hot extreme events and less cold extreme events. While it is clear that the increase in mean temperature will result in more hot extreme events, it is not apparent what will happen to other atmospheric variables such as Convective Available Potential Energy (CAPE) and wind shear. Possible impacts of an increasing mean temperature include the ability of the atmosphere to hold more moisture. This may lead to an increase in CAPE and thus stronger convection. While an increasing maximum surface temperature may lead to an increase in CAPE and in turn an increase in convection, increasing temperature aloft may lead to an increase in static stability, a decrease in CAPE and thus less convection.

Severe convective weather (thunderstorms, hail, tornadoes, etc) are relatively rare atmospheric phenomena, yet wield a high impact on any location that may experience them. Figures 1.3.1 – 1.3.2 and 1.4 show the number of fatalities, number of injuries, and cost of damage for the decade 1997 to 2006 in the United States. These data were collected from the official yearly summaries of natural hazard statistics compiled by the National Weather Service. Between 1997 and 2006 there

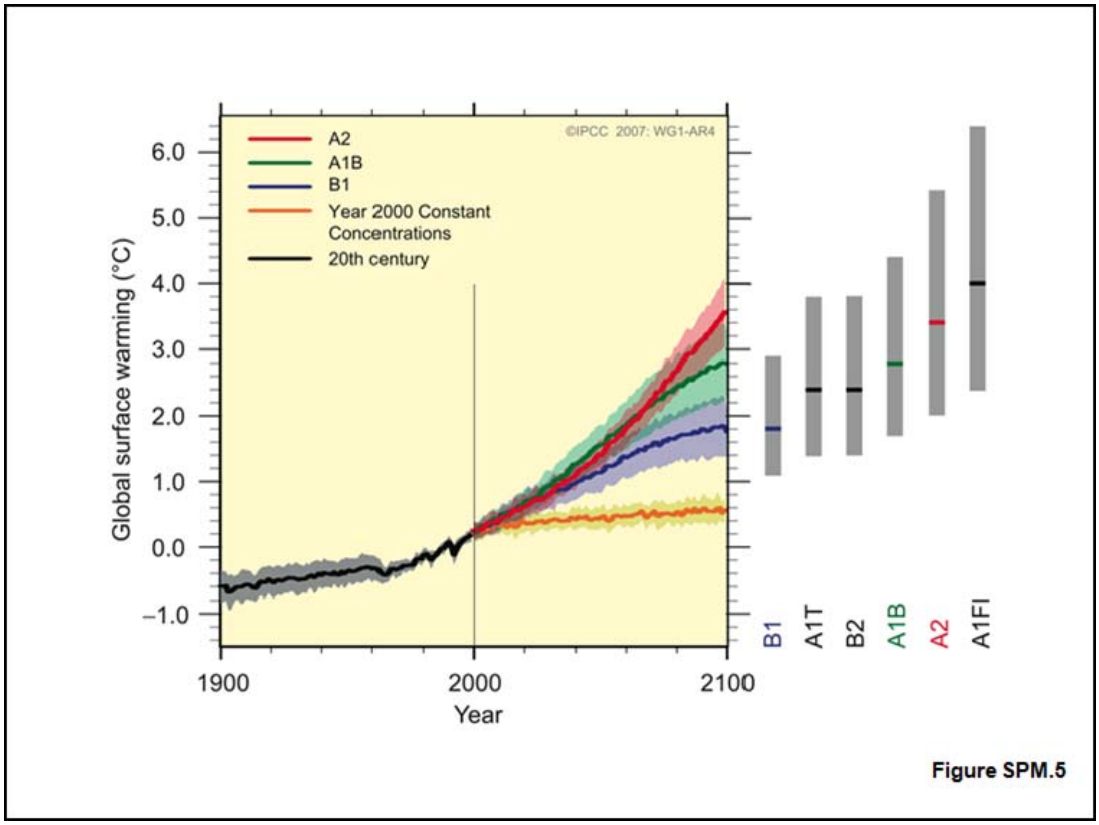


Fig. 1.1: Solid lines are multi-model global averages of surface warming (relative to 1980–1999) for the scenarios A2, A1B and B1, shown as continuations of the 20th century simulations. Shading denotes the ±1 standard deviation range of individual model annual averages. The orange line is for the experiment where concentrations were held constant at year 2000 values. The grey bars at right indicate the best estimate (solid line within each bar) and the likely range assessed for the six SRES marker scenarios. The assessment of the best estimate and likely ranges in the grey bars includes the AOGCMs in the left part of the figure, as well as results from a hierarchy of independent models and observational constraints. Image reproduced from "Summary for Policy Makers" (SPM) of IPCC AR4 Working Group 1 (IPCC, 2007)

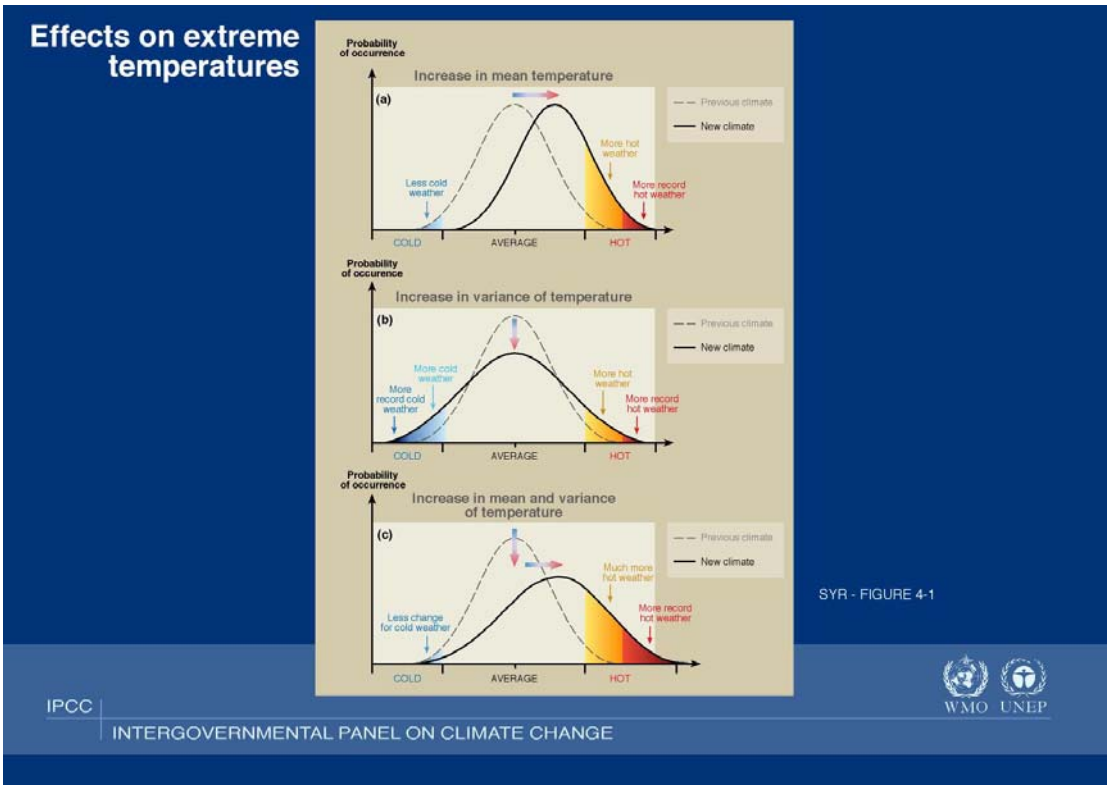
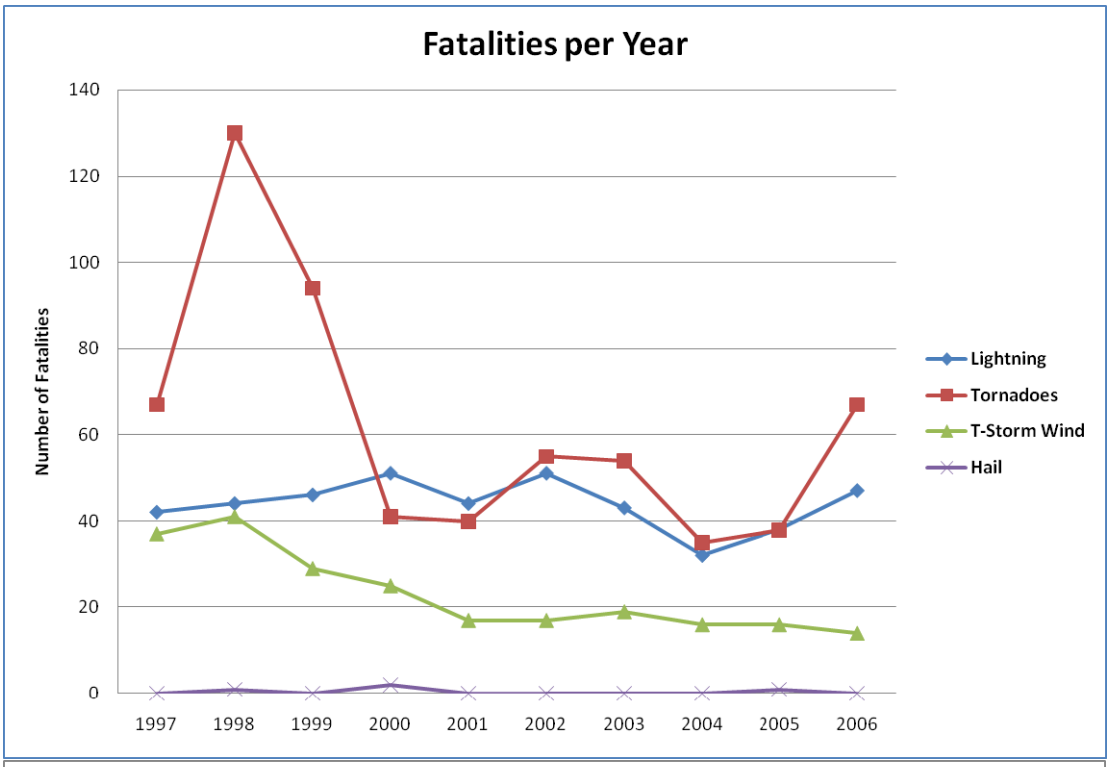


Fig. 1.2: Effects of increasing global mean temperature on extremes. The top image shows the effect for only increasing the mean. The middle image shows the effect for only increasing the variance. The bottom image shows the combined effect of increasing both the variance and the mean. Image taken from the graphics section of the IPCC website (http://www.ipcc.ch/present/graphics.htm)



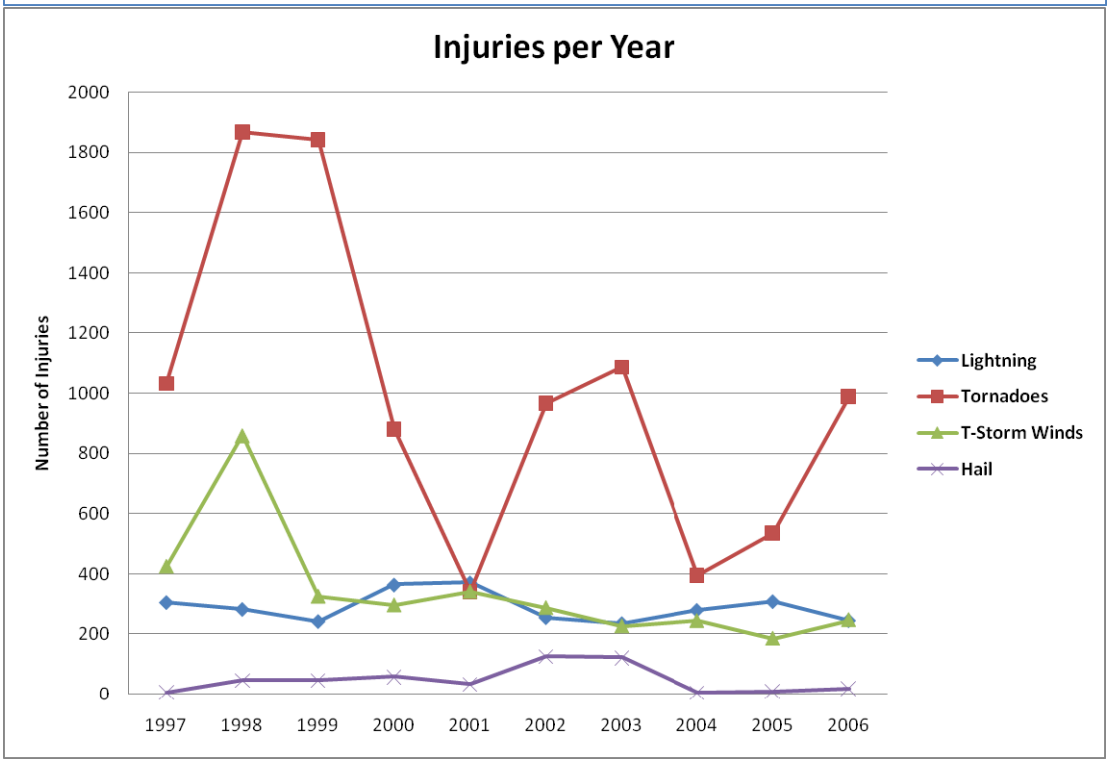


Fig 1.3: Effects of convective weather on life from 1997 to 2006. Fig. 1.3.1 shows the number of fatalities per year while Fig 1.3.2 shows the number of injuries per year. Data courtesy the National Weather Service's yearly Summary of Natural Hazard Statistics.

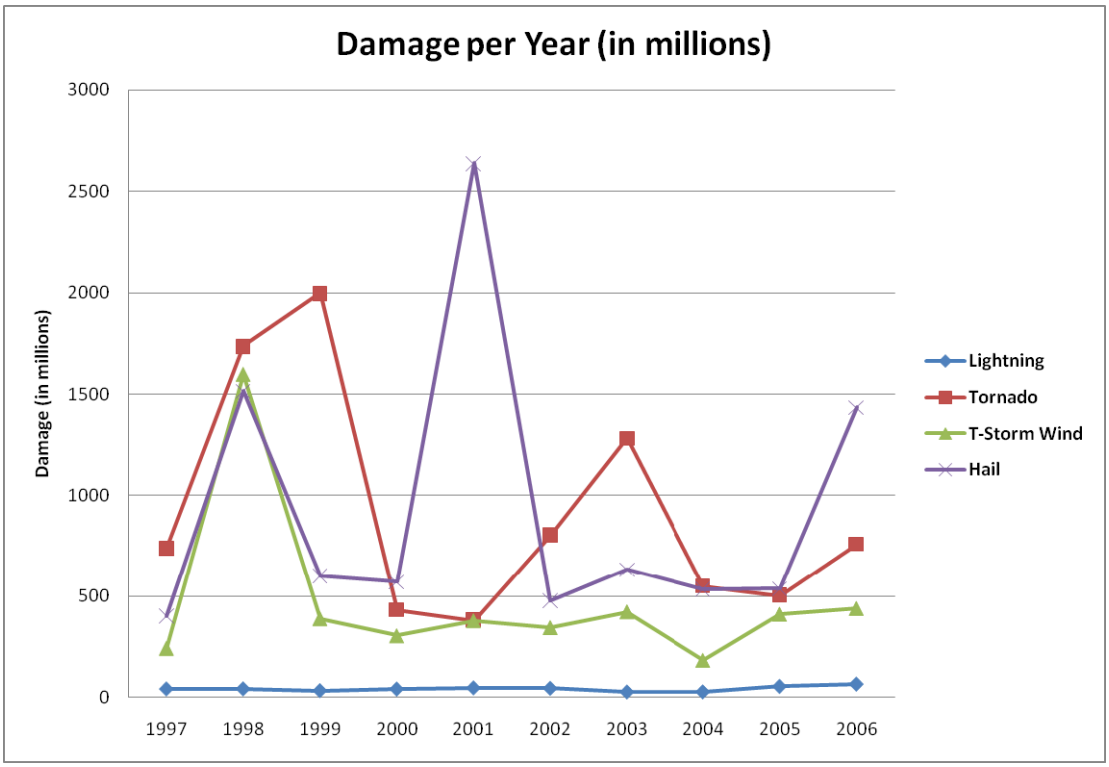


Fig 1.4: Damages (in millions of dollars) relating to convective weather from 1997 to 2006. Data courtesy the National Weather Service's yearly Summary of Natural Hazard Statistics.

have been at least 1294 fatalities, 16,734 injuries, and over $23 Billion in damages as a direct result of convective weather.

The impacts of global warming on such severe convective weather are poorly understood at best. Before making a prediction on how global warming will impact severe convective weather, current climatologies of severe convective weather must be properly understood. As previously mentioned, severe convective weather events are relatively rare but high impact atmospheric phenomena at any location due to their very small temporal and spatial scales. Consequently, assessing climatologies of actual severe convective weather events is difficult. Inconsistencies in reporting criteria and improvements in the technology used to observe severe weather make the problem of developing reliable long-term climatologies of severe weather events nearly impossible (Brooks and Doswell, 2001; Doswell et al., 2005).

Brown and Murphy (1996) and Brooks et al. (2003) proposed the use of covariates that represent the severe weather environment as proxies for the occurrence of weather events that could not be accurately quantified. Environmental conditions conducive to the occurrence of severe weather can be quantified from meteorological soundings in terms of the convective available potential energy (CAPE) and vertical shear of the horizontal wind. In each of the studies, extreme values of the covariates were closely related to the average occurrence of severe weather. In the context of establishing climatologies of severe convective weather events, the problem is transformed from trying to assess an inherently inadequate database of observed severe convective weather events to trying to establish a

relationship between better observed environmental conditions and the original events in question.

It has been shown that most convective parameters derived from the NCAR / NCEP global reanalysis (hereafter referred to as simply reanalysis) are qualitatively similar to convective parameters derived from observed soundings (Lee 2002). Niall and Walsh (2005) showed that CAPE calculated from reanalysis showed a strong relationship to hail incidents. Brooks et al. (2003) calculated CAPE values using the mixed layer within the lowest 100 hPa of the atmosphere and shear values over the 0-6 km range (hereafter referred to as deep layer shear). They concluded that the higher the CAPE and shear, the greater the probability became that the environmental conditions would be associated with severe convective weather. This is consistent with the results of Rasmussen and Blanchard (1998) who used observed environmental parameters from neighboring meteorological soundings. One caveat mentioned by Brooks et al. (2003) is that the difference in tornadic and non-tornadic environments is harder to differentiate in the reanalysis environments than observed environments.

Brooks et al. (2007) explored the annual cycle of the severe convective weather environments from the reanalysis. Qualitatively, it was found that the reanalysis data capture the spatial and temporal variability observed in the United States (Brooks et al., 2003; Doswell et al., 2005.). Brooks et al. (2003) concluded that the central part of the United States was the region with the most frequent number of days with favorable severe convective weather environments (Figure 1.5). This qualitative ability to recreate severe convective weather environments from the

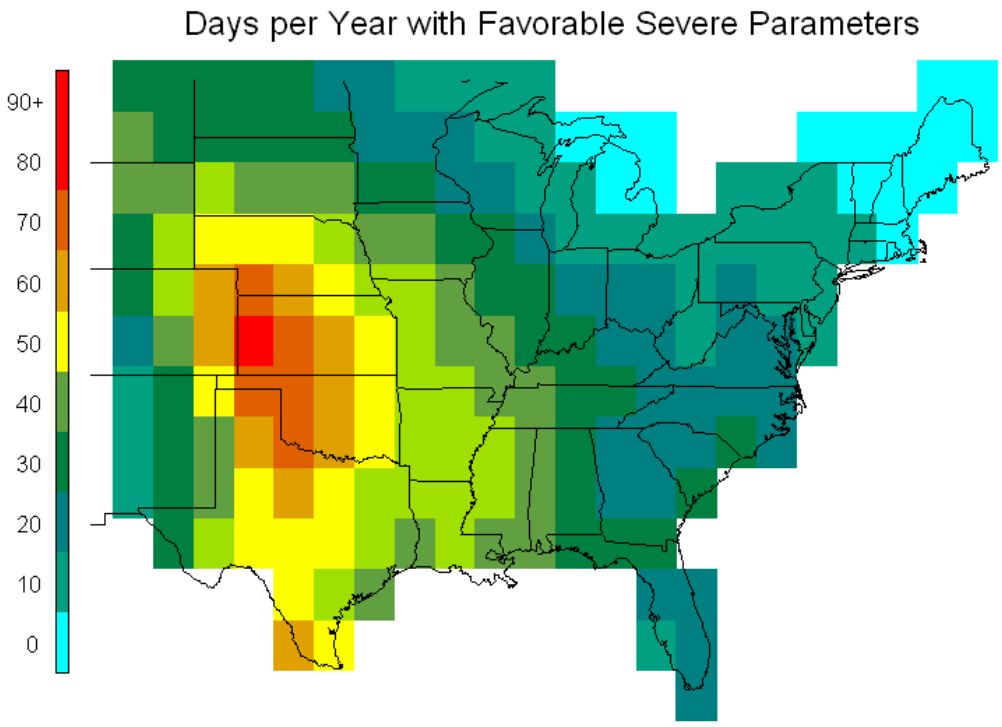


Fig. 1.5: The number of days per year with favorable severe parameters for severe convection. Note the maximum over the central plains of the United States. Image courtesy of Harold Brooks (personal communication).

reanalysis data points towards the possibility that atmospheric models of similar resolution should be capable of doing the same.

Typically, assessments of possible climate change impacts resulting from changes in anthropogenic forcing are based on or derived from global climate models. Previously, analyses derived from global climate models have had too coarse a resolution – on the order of greater than two hundred kilometers - to simulate severe convective weather environments. The resolution of these global climate models is even too coarse to adequately simulate mesoscale environments.

Due to the inadequacies of previous global climate models, the IPCC (Houghton et al., 2001) has been unable to reach conclusions on climate change projections for severe weather due to anthropogenic forcing. The IPCC's Third Assessment's chapter on model projections of future climate change, specifically the subsection on precipitation and convection, states

> "Although of great importance to society for their potential for causing destruction, as well as their human and economic impacts, there is little guidance from AOGCMs concerning the future behavior of tornadoes, hail or lightning. This is because these phenomena are not explicitly resolved in AOGCMs, and any studies that have been done have had to rely on empirical relationships between model features and the phenomenon of interest…However, there have been no recent studies examining this problem with the current generation of global climate models. Due to the fact that these severe weather phenomena are sub-grid scale (even more so than discussed below for tropical cyclones), and that second and third order linkages between model output and empirical relationships for limited regions must be used to derive results, we cannot reach any definitive conclusions concerning possible future increases in hail and lightning, and there is no information from AOGCMs concerning future changes in tornado activity."
>
> (Cubasch et al., 2001)

Recent improvements in global climate model resolution, and the declining cost of output storage, have promoted the archiving of high resolution model output. Currently, several runs of the high resolution NCAR Community Climate System Model version 3 (CCSM3) are archived at six hour resolution, twenty-six vertical levels, and approximately 1.4 degree horizontal resolution, which is on the order of the same horizontal resolution of the global reanalysis.

Even with the advances made in global climate models, these models are still incapable of resolving actual severe weather events, as these events occur at scales that are still well below the horizontal resolution within global climate models. As a result, assessing the distribution of severe weather within a global climate model is still limited to assessing environments associated with severe convective weather. An assessment is presented of how the CCSM3 global climate model represents severe weather environments. It is proposed that the severe weather environments simulated by this new generation of high resolution climate models compares sufficiently well with reanalysis based severe weather environments. Furthermore, changes between future and present severe weather environments simulated by global climate models are expected to be significant and useful for guidance on future changes in severe weather occurrence.

Results are presented from an investigation of the ability of the CCSM3 to simulate severe convective weather environments of North America. A description of the CCSM3 model is presented in the next section, followed by a discussion of the methods used to analyze the model simulations and to compare the model output with the reanalyses. In chapter 4, the model severe weather environments for the period

1980-1999 are compared with the severe weather environments from reanalysis data discussed in Brooks et al. (2003). Additionally, results are shown from an investigation of the CCSM3 simulated future severe weather environment for the period 2080-2099 under a high anthropogenic greenhouse gas and aerosol emissions scenario (but not the highest scenario). A comparison of the CCSM3 simulated current environment to the CCSM3 future simulated environment is shown.

Chapter 2: Description of the Models

2.1 Community Climate Systems Model 3 (CCSM3)

The CCSM3 is a coupled global climate model consisting of atmosphere, land surface, sea-ice, and ocean components (Collins et al., 2006) developed at the National Center for Atmospheric Research (NCAR). Each component is a model in itself joined together through a flux coupler. Each component only exchanges information with the flux coupler, and has no direct connection to any other components. In general, any flux field is computed once in one component on that component's model grid and is then made available to the other components via the flux coupler for use as boundary forcing information.

The archived high resolution runs include a preindustrial control run initialized in 1870 (constant external climate forcing as observed in 1870), a present day control run initialized in 1990 (constant external climate forcing as observed in 1990), a 20th century simulation (containing the observed changes of greenhouse gases, sulphate aerosols, volcanic aerosols, and solar irradiance from the 20th century), and 21st century "future scenarios" (containing estimated changes in greenhouse gas and aerosol concentrations, but fixed values of solar irradiance and fixed background stratospheric volcanic aerosol amounts). For this particular study, a 20th century simulation initialized in 1870 and run through the 20th century (model run b30.030e) was chosen in an effort to assess how well climate models can simulate current severe weather environment. A 21st century simulation initialized in 2000 (from the 31 Dec 1999 conditions at the end of the 20th century simulation) and run through the 21st century (model run b30.042e - part of the A2 emissions scenario

family) was chosen in an effort to assess the simulated severe weather environment of a future under global warming.

The A2 future emissions scenario is an IPCC high greenhouse gas and anthropogenic aerosol emission scenario, but not the highest. The storyline for this scenario family is based on a "heterogeneous world with continuously increasing global population and regionally oriented economic growth that is more fragmented and slower than in other storylines" (Nakicenovic et. al, 2000). The IPCC A2 emission scenario ensemble projects an increase in future global mean surface temperatures of 3.1°C, with the CCSM3 being in the lower half (~30%) of this ensemble (IPCC, 2001). This emission scenario was chosen in an effort to look for a possible signal on the effect of global warming on severe convective weather environments. If a signal cannot be found in this, a high emission scenario, the likelihood of finding a signal in a lesser emission scenario is is significantly reduced.

The atmospheric portion of the CCSM3, the Community Atmospheric Model 3 (CAM3), is a spectral model with 85-wavenumber triangular truncation (approximately 1.4 degree at the equator) in the horizontal with 26 terrain following hybrid levels in the vertical. The numerical scheme used in the CAM3 is an Eulerian spectral transform, with semi-Lagrangian tracer transport with semi-implicit leapfrog time stepping (Collins et al., 2006). CAM3's vertical resolution contains 4 levels below 850 hPa and 13 levels above 200 hPa (topmost being 2.2 hPa). Several runs of this model have output fields archived every 6 hours.

The land-surface portion of the CCSM3, the Community Land Model 3 (CLM3) uses a horizontal resolution of identical to that of the CAM3 (Vertenstein et

al., 2004) and 10 levels (soil layers) in the vertical (Oleson et al., 2004). The oceanic portion of the CCSM3 is an extension of the Parallel Ocean Program (POP) from Los Alamos National Laboratory (LANL). Currently version 1.4.3 of this model is currently included in the CCSM3. This model uses a grid resolution of approximately 1° in the horizontal and 40 levels in the vertical with the North-Pole centered over Greenland (Vertenstein et al., 2004). The sea-ice portion of the CCSM3, the Community Sea-Ice Model 5 (CSIM5) is a fully dynamic ice model that uses an identical grid as the POP ocean model (Vertenstein et al., 2004).

In assessing a model's ability to simulate realistic severe weather environments, the convective scheme used for deep convection within the model is of utmost importance. The CAM3 uses the Zhang – McFarlane convective scheme for deep convection (Collins et al., 2006) which is similar to a simplified Arakawa – Schubert convective scheme (Zhang and McFarlane, 1995). In the NCAR technical note titled "Description of the NCAR Community Atmosphere Model (CAM 3.0)" the following description of the Zhang – McFarlane convective scheme is found.

> "The process of deep convection is treated with a parameterization scheme developed by Zhang and McFarlane [1995]. The scheme is based on a plume ensemble approach where it is assumed that an ensemble of convective scale updrafts (and the associated saturated downdrafts) may exist whenever the atmosphere is conditionally unstable in the lower troposphere. The updraft ensemble is comprised of plumes sufficiently buoyant so as to penetrate the unstable layer, where all plumes have the same upward mass flux at the bottom of the convective layer. Moist convection occurs only when there is convective available potential energy (CAPE) for which parcel ascent from the sub-cloud layer acts to destroy the CAPE at an exponential rate using a specified adjustment time scale"
>
> (Collins et. al, 2004)

The technical note further states the adjustment time scale for the relaxation period is 7200s. The Zhang-McFarlane scheme is a relatively simple convective scheme that does better over the tropics than over the mid-latitudes (Shafer, personal communication).

1.2 Reanalysis Data

Through cooperation between NCAR and the National Centers for Environmental Prediction (NCEP) a dataset of global analysis of atmospheric variables has been created (Kalnay et al., 1996). By combining data assimilation of available observational data with near term model forecasts information from regions with dense observational networks can be transported to regions with little if any observations (particularly oceans). In essence, this is done by

“

1. “Recovering all available observations from each time index and synthesizing them with a static data assimilation system.
2. Using the observational fields to initialize a model for a 6-h forecast. The model used (hereafter referred to as the reanalysis model) was identical to the NCEP global operational model, except for the horizontal resolution. The reanalysis model is T62 (equivalent to a horizontal resolution of approximately 210 km), while the operational model is T126 (approximately 105 km).

3. Using the forecast as a first-guess, in conjunction with concurrent observational fields, to construct the reanalysis output. Reanalysis fields were generated with an optimal interpolation technique.
4. Repeating the process every 6 h."

(Brooks et. al, 2003)

The horizontal resolution of the reanalysis data is 1.875º in the longitude and 1.915º in the latitude. This is approximately 200 km grid spacing over most of the globe. The vertical resolution consists of 28 levels in the vertical, with approximately 10 levels below 700 hPa. The similarities in resolution make the reanalysis data an appropriate benchmark for comparing CCSM3 output.

Chapter 3: Methodology

3.1 Calculation of Atmospheric Variables

For the reanalysis data, atmospheric variables needed for this analysis were computed by Brooks et al. (2003). Communication with the authors of that paper yielded access to their dataset. The CAPE and deep layer shear found within that dataset were computed using a version of the Skew-t/Hodograph Analysis and Research Program (SHARP) (Hart and Korotky, 1991). It should be noted that the CAPE computed by SHARP was computed from a surface parcel 100 hPa deep with potential temperature and moisture averaged over the depth of this parcel (Brooks et al., 2003).

Attempts to follow the Brooks et al. (2003) methodology exactly proved unsuccessful. The CCSM3 archived output does not include the CAPE field. To compute the CCSM3 CAPE field, two routines included in NCAR Command Language (NCL) are available: rip_cape_2d and rip_cape_3d. Both routines take arrays ordered top to bottom of pressure, temperature, geopotential height and mixing ratio as well as arrays of surface pressure and surface geopotential. Since the CAM3 uses hybrid levels in the vertical a separate NCL routine was used to convert the hybrid pressure levels to true pressure levels needed for the pressure level array in both routines. It should be noted that in both routines CAPE is computed using the model output's vertical grid and not interpolated.

The difference between these two CAPE routines lies in what parcel is used to compute the positive buoyancy. In the rip_cape_2d routine, the parcel refers to a 500 meter deep layer centered on the model level with the maximum equivalent potential

temperature. Furthermore, this parcel has potential temperature and mixing ratio, from the model, averaged over its entirety. In the rip_cape_3d routine, the parcel refers to each vertical level with potential temperature and mixing ratio averaged over a depth of 500 meters centered on that level. Thus, the rip_cape_2d routine generates one CAPE value for each horizontal grid point whereas the rip_cape_3d routine generates 26 CAPE values – one for each vertical level – for each horizontal grid point. Neither of the methods of computing CAPE are equivalent to the method of Brooks et al. (2003), however using the model layer closest to the surface from the rip_cape_3d routine provides the most similar parcel to the Brooks et al. (2003) parcel.

Additionally, Figure 3.1 shows a comparison between the rip_cape_2d routine and the rip_cape_3d indicated CAPE values computed by the rip_cape_2d routine were consistently less than CAPE values produced by the rip_cape_3d routine. This makes little physical sense as CAPE computed from the parcel with maximum theta-e in the column should always be greater than or equal to the CAPE computed from the surface based parcel. Thus the CAPE values computed from the rip_cape_2d routine were discarded as potentially erroneous and the analyses proceeded with exclusive use of the rip_cape_3d routine.

The CCSM3 archived output also includes the U and V components of the wind. Once again, this output is stored on hybrid levels, not physical height. Thus to calculate the deep layer (0 – 6 km) shear, the output was converted from hybrid levels to geopotential to height using built in routines of NCL. Since the 6 km wind did not always fall on one of the 26 vertical levels, a linear interpolation routine within NCL

was used to interpolate the U and V wind components to an exact height of 6 km AGL.

Due to computational complexities in converting the U and V wind components to physical height coordinates it was once again impractical to compute the same deep layer shear from the model output as was used in Brooks et al. (2003). These complexities include, but are not limited to, the fact that linear interpolation was used to compute the 6 km wind and that the wind at the lowest model level is potentially significantly different than the surface model wind. Thus, it was decided to use the 6 km wind as an approximation for the model deep layer shear. This differs from the deep layer shear computed from Brooks et al. (2003) which uses 6 km and surface winds to compute deep layer shear values.

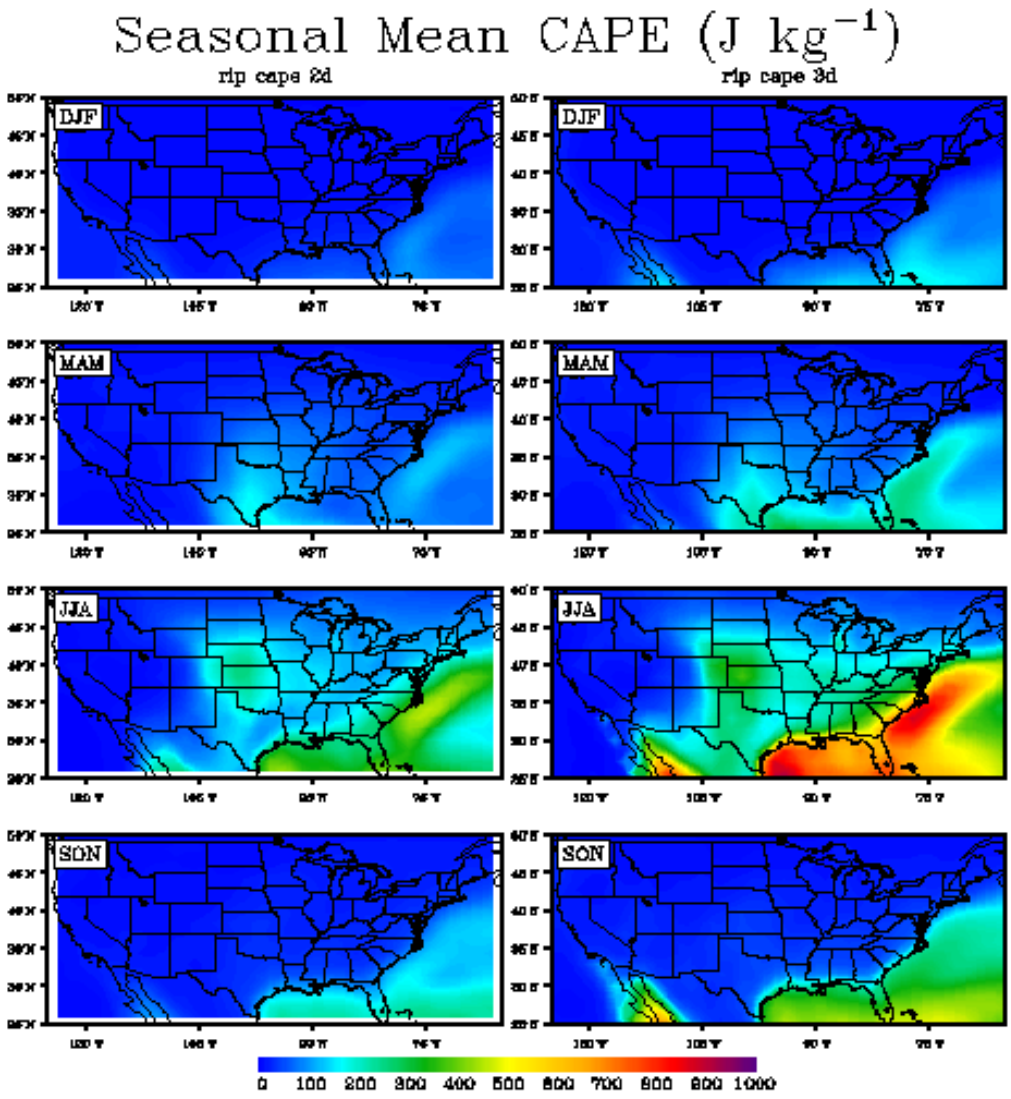


Fig 3.1: Mean CAPE values by season for both the rip_cape_2d (left column) and rip_cape_3d (right column) routines. Note the higher values when using the rip_cape_3d. Output is averaged over 20 years.

3.2 Analysis of CCSM3 Severe Weather Environment

As previously mentioned, Brooks et al. (2003) demonstrated the effectiveness of using environmental covariates derived from the reanalysis data in assessing the severe weather environment of the reanalysis - essentially mimicking the traditional proximity sounding analysis paradigm. This was achieved by comparing reanalyses fields to observations for known severe weather environments. Building on this success, an analysis of the severe weather environment with the CCSM3, and more specifically the CAM3, will be carried out here in a similar manner.

The reanalysis data is derived from real observations made every 6 hours and therefore has some semblance of reality. For example, reanalysis data for 21 July 1983 should correspond to observational data for 21 July 1983. This same relation between observational data for a specific date and model output for the 20th century runs of CCSM3 cannot be made.

The 20th century runs of the CCSM3 were initialized in 1870 and while changes in anthropogenic forcing corresponding to observations are updated every model year, the fact still remains that the initial conditions were based on conditions in 1870. This means that there is no resemblance of specific model day 21 July 1983 to observed day 21 July 1983 apart from the general external radiative forcing conditions for that date, such as solar irradiance, greenhouse gases, and sulphate and volcanic aerosols. This is a critical distinction to make as it means the analysis of CCSM3 cannot be carried out in the exact manner the analysis of the reanalysis data was performed.

Since comparison of CCSM3 model years to observational years cannot be made, this leads to a fundamental question – given that there is no 21 July 1983 in the model, how does one determine if the model environments are reasonable? In an effort to address this fundamental question, analysis of model distributions will be carried out in a variety of ways and scales. This will include comparisons of the model output with reanalysis data over an entire North American domain, as well as a sub-domain centered over the central United States in both yearly, seasonal and decadal time scales. CAPE will be investigated in both its own dimension as well as in joint distributions of CAPE and deep layer shear. If the model output statistics are qualitatively similar to those of the reanalysis it can be said that the model produces reasonable environments.

The analysis of the future severe weather environment as simulated by the CCSM3 is conducted in a similar manner as that of the analysis of the current severe weather environment simulated by the CCSM3. The difference is that comparisons will be made between the simulated future severe weather environment and the simulated current severe weather environment – not between model and reanalysis.

It cannot be stressed enough that it is not necessary to get the absolute magnitudes of CAPE and deep layer shear correct when compared to the reanalysis data for this analysis to provide useful information. Therefore, the analysis is heavily biased toward comparisons of relative terms.

Chapter 4: Current Climate Simulation

4.1 Results from CCSM3 20th Century Simulation

The CCSM3 spatial distribution of seasonal mean CAPE (zero CAPE included) is shown in Figure 4.1. During winter (Dec – Feb) there is less than 50 J kg^{-1} of mean CAPE across the entire region, with the exception of the southern Gulf of Mexico to the Gulf Stream, where slightly higher values are found. In spring (Mar – May), mean CAPE values increase throughout the southern plains with a nose of higher mean CAPE values across the western Gulf of Mexico into south central Texas. At the same time, the Gulf Stream continues to show higher values than surrounding areas. Summer (Jun – Aug) shows much of the eastern two-thirds of the United States having mean CAPE values of greater than 100 J kg^{-1}. Their are two areas most noticeable: the relative maximum in the north central plains and the absolute maximum located off the Mid-Atlantic United States, again, over the Gulf Stream. By autumn (Sep – Nov), much of the United States once again have mean CAPE less than 50 J kg^{-1}, the exception being those regions near the Gulf of Mexico and Atlantic coasts.

While the values of mean CAPE are lower in the CCSM3 than in the reanalysis data, the spatial distribution are qualitatively similar (Figure 4.1). Both datasets capture relative maximum in mean CAPE over the Kansas – Nebraska area in summer. Some notable discrepancies in the clack of large mean CAPE values over the Gulf Stream in the reanalysis data, and larger spatial area of mean CAPE over the southern plains in autumn in the reanalysis data.

The above comparison of seasonal mean CAPE values between the CCSM3 and the reanalysis data indicates that the CCSM3 accurately captures the spatial distribution of mean CAPE. The same cannot be said of the CCSM3's ability to reproduce the magnitude of the mean CAPE. A significant exception to this is areas near and over regions of warm water, in particular the Gulf Stream Current. Mean CAPE values over the Gulf Stream Current are considerably higher than mean CAPE values over the rest of the domain. The reanalysis does not show this propensity for higher mean CAPE values over warm water indicating this may be a bias of the CCSM3.

As previously mentioned, the reanalysis data are averaged over a time period of 42 years while the CCSM3 output is averaged over only 20 years. Additionally, the number of gridpoints in the North American domain (25ºN to 50ºN and 125ºW to 65ºW) isn't equal in the reanalysis and CCSM3 output. In an effort to accurately compare the frequency distribution of the CAPE values between the CCSM3 and reanalysis the following normalization technique was employed on each dataset.

1. Count the number of occurrences of CAPE values in specific ranges for all 6-hour time periods for all gridpoints in the domain
2. Divide the resulting value by the number of gridpoints in the domain.
3. Divide the resulting value by the number of years contained in the time period of each dataset.

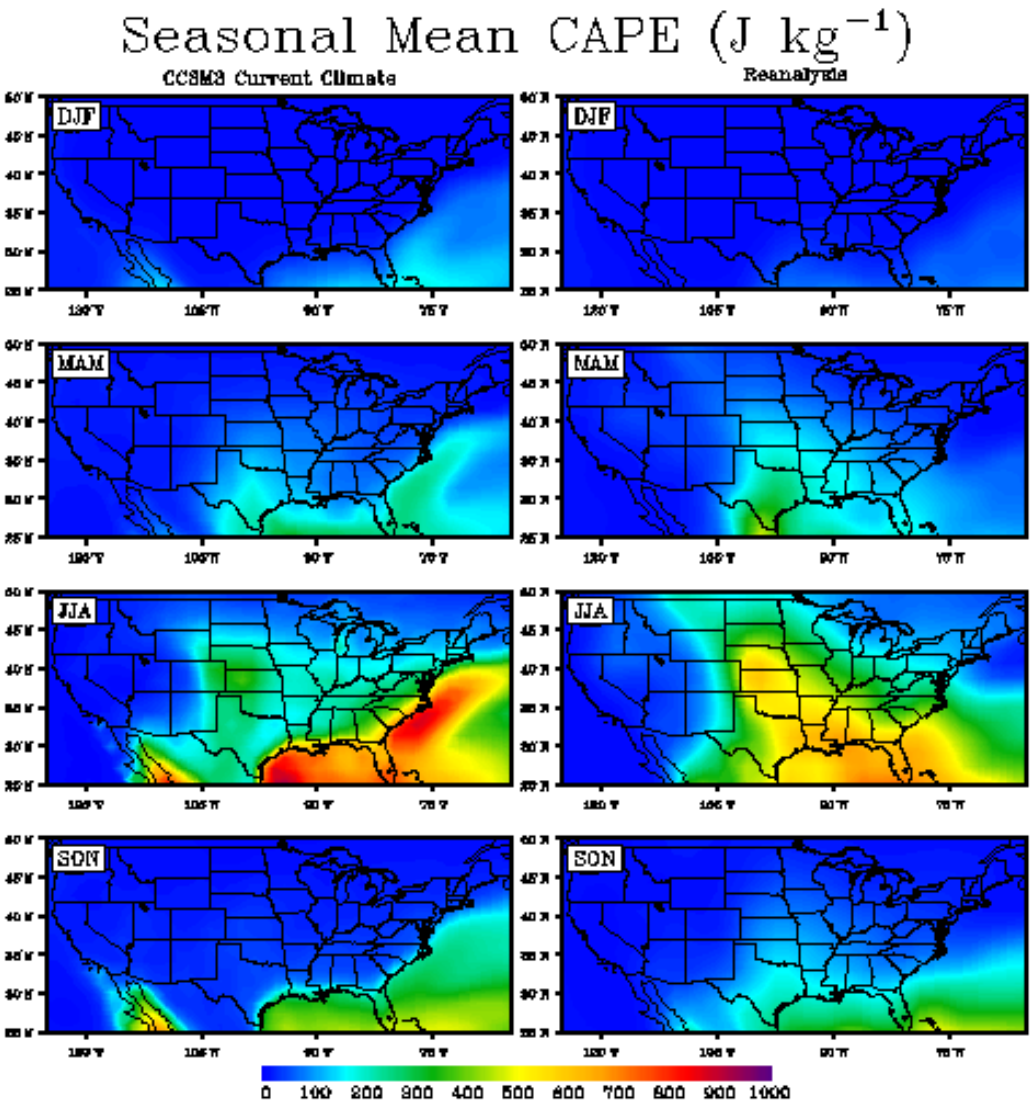


Fig 4.1: Mean CAPE values by season for both the CCSM3 current simulation (left column) and the Reanalysis (right column). Note that the CCSM3 output is averaged over 20 years while the Reanalysis is averaged over 42 years.

Normalization by this technique produces a mean frequency distribution for a single gridpoint of CAPE values for one year at 6 hour time intervals. This allows for direct comparison of CAPE values between the CCSM3 and the reanalysis.

Using the aforementioned normalization process, a frequency distribution of CCSM3 CAPE and reanalysis CAPE was created for the whole North American domain shown in Fig. 1 in log - CAPE space (Figure 4.2). Log – CAPE space was chosen to emphasize the regions of higher CAPE, which are more important when investigating convection. Both distributions are bimodal with a small peak less than a 100 J kg^{-1} and the primary peak between 500 J kg^{-1} and 1000 J kg^{-1}. For all CAPE values less than $10^{2.2}$ (~ 160) J kg^{-1} the CCSM3's frequency of occurrence is roughly half that of the reanalysis. The reanalysis peaks first between $10^{1.4}$ and $10^{1.6}$ (~ 25 and 40) J kg^{-1} and while the CCSM3 peaks slightly higher between $10^{1.6}$ and $10^{1.8}$ (~ 40 and 60) J kg^{-1}. It is important to point out that the maximum peak that occurs in the higher CAPE regions is an artifact of working in log – CAPE space. In linear space the maximum would occur in the lower CAPE region and the distribution would like a Weibull distribution – a peak occurring in low CAPE environments and an exponential decrease in frequency of occurrence with increasing CAPE.

As with CAPE values less than 100 J kg^{-1}, CCSM3 CAPE values greater than 100 J kg^{-1} peak at higher values than the reanalysis; however, the maximum frequency of occurrence for the CCSM3 remains less than that of the reanalysis.

Toward the primary peak, the CCSM3's frequency of occurrence becomes much closer to that of the reanalysis – even surpassing it for CAPE values greater than 102.8 (~ 630) J kg^{-1}. The skewness of the CCSM3 frequency distribution toward

higher CAPE values is most likely the result of a warm water bias on CAPE values discussed previously.

This warm water bias that shows up in the Gulf and the Gulf Stream makes a comparison of frequency distributions regions containing water extremely difficult. In an attempt to lessen, or even remove, the impact of any biases in distributions introduced by warm water, a region of the central United States (30°N to 45°N and 105°W to 90°W) was chosen for further investigation.

The normalized frequency distributions in Figure 4.3 show a qualitatively similar pattern between the CCSM3 and reanalysis distributions. Each has a peak between $10^{2.8}$ and 10^{3} (~630 and 1000) J kg^{-1} and gradually increase to that peak and then quickly falls off for both distributions. Differences between the two distributions include a reanalysis increase by a factor of 4 between CAPE values of 10 J kg^{-1} and 1000 J kg^{-1} while the CCSM3 increase is only by a factor of 2. Additionally, the CCSM3 frequency takes longer to decrease than the reanalysis after peaking around 1000 J kg^{-1}.

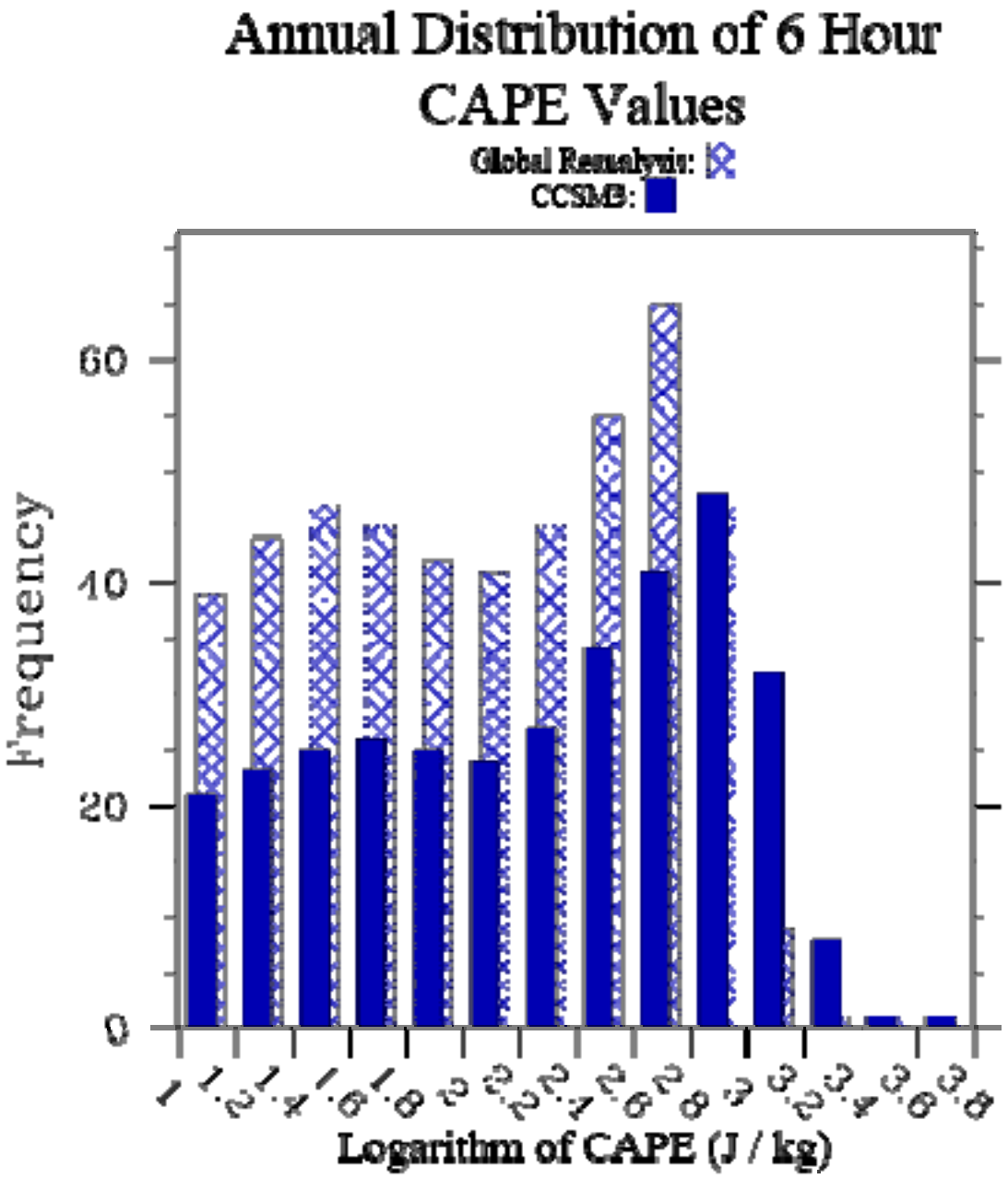


Fig. 4.2: Annual distribution of 6 hour CAPE values for the entire North American domain in log – CAPE space. CCSM3 output is solid while reanalysis data is checkered

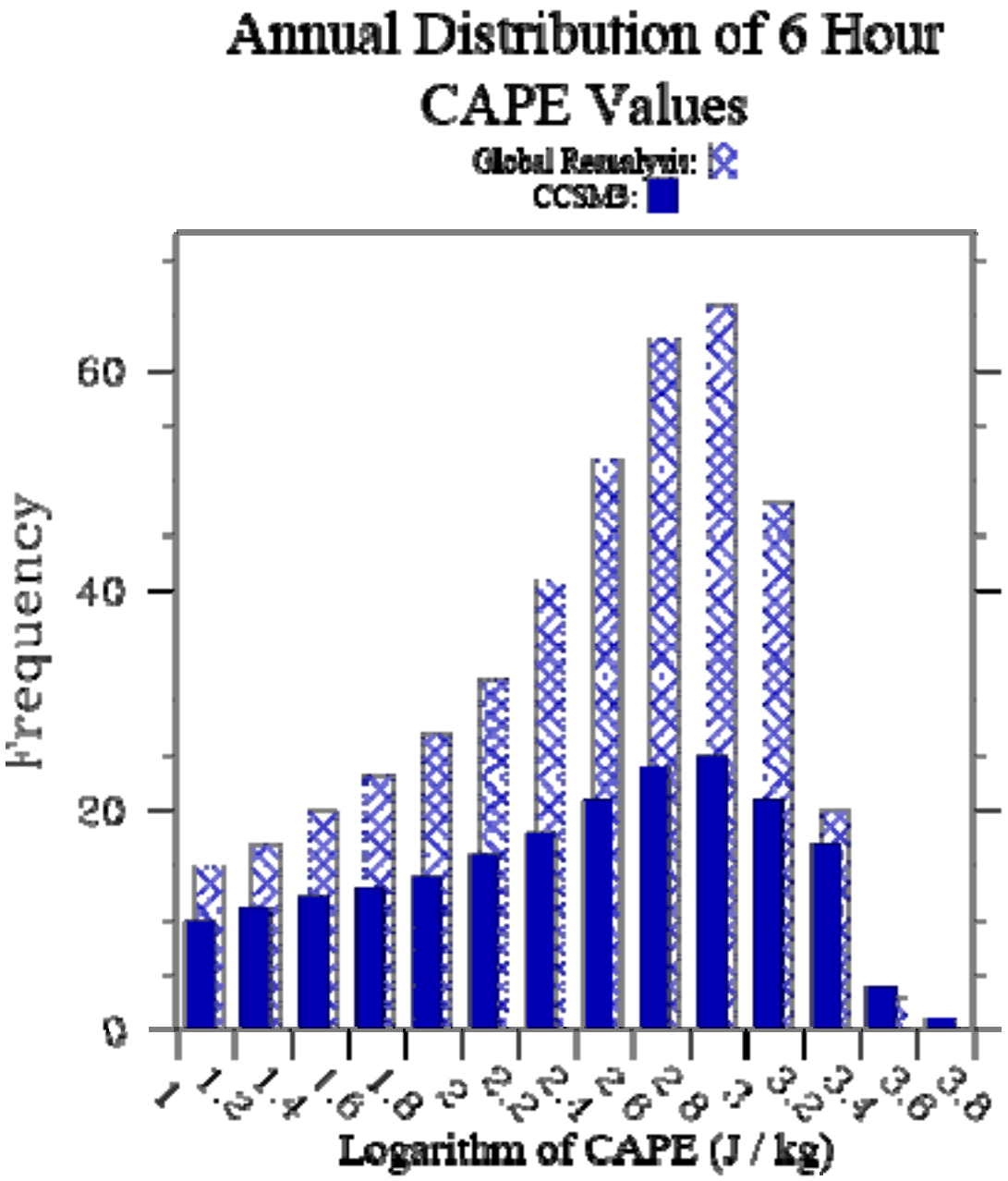


Fig. 4.2: Annual distribution of 6 hour CAPE values for the central United State in log – CAPE space. CCSM3 output is solid while reanalysis data is checkered

Modifying slightly Brooks et al. (2003) best discriminator between significant severe thunderstorm environments and other environments, the product of CAPE and deep layer shear greater than 10,000 m3s-2 was used to discriminate between significant severe thunderstorm environments and other environments in the CCSM3. A CAPE – deep layer shear normalized joint distribution plot for the central United States was created showing the annual frequency of CAPE and deep layer shear values in log CAPE – log deep layer shear space and is shown in Figure 4.4. This distribution exhibits a similar structure as the CAPE distribution – a small peak at relatively low CAPE and high shear and a larger peak at high CAPE and lower shear. The CAPE – deep layer shear normalized joint distribution plots for both the reanalysis data (Figure 4.4) and CCSM3 exhibit an absolute maximum in the region with high CAPE and lower shear, albeit the CCSM3 has considerably lower frequency than the reanalysis.

The spatial distribution of the annual number of 6-hourly periods with the product of CAPE and deep layer shear greater than 10,000 $m^3 s^{-3}$ in Figure 4.5 reveals a relative maximum located over the central plains of the United States. It is

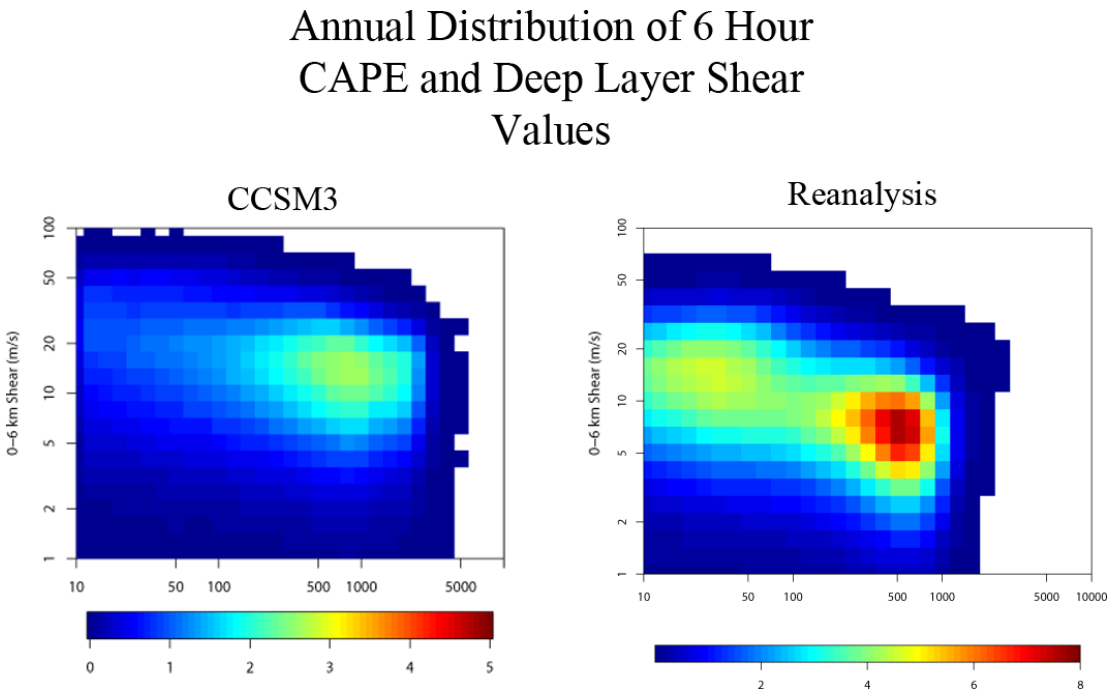


Fig 4.4: Normalized joint distribution plot of CAPE and deep layer shear for the central United States. The CCSM3 output is on the left and the reanalysis is on the right.

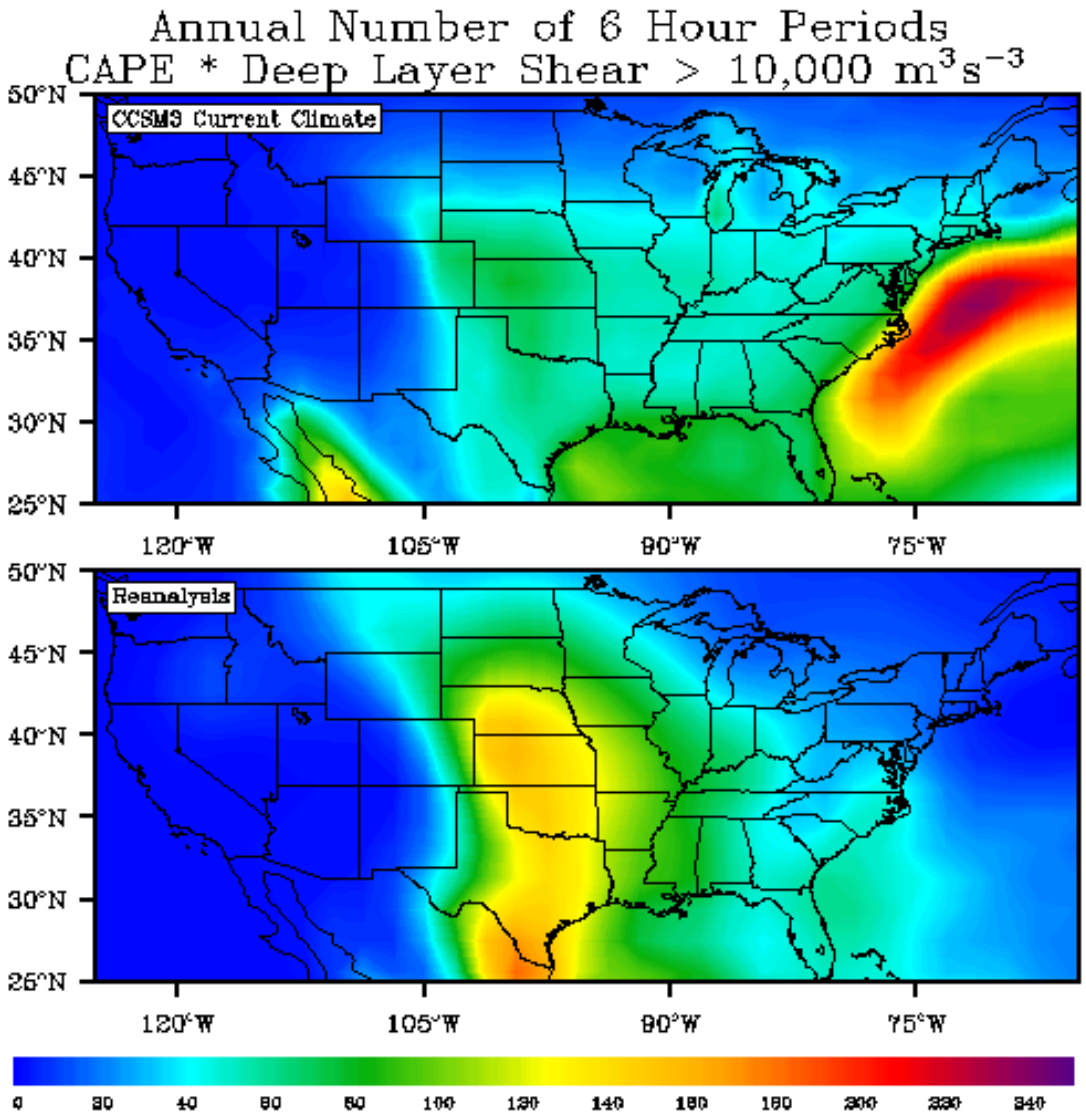


Fig 4.5: Annual number of 6 hour periods with environments favorable for severe convective weather. The CCSM (left) is averaged over 20 years while the reanalysis (right) is averaged over 42 years.

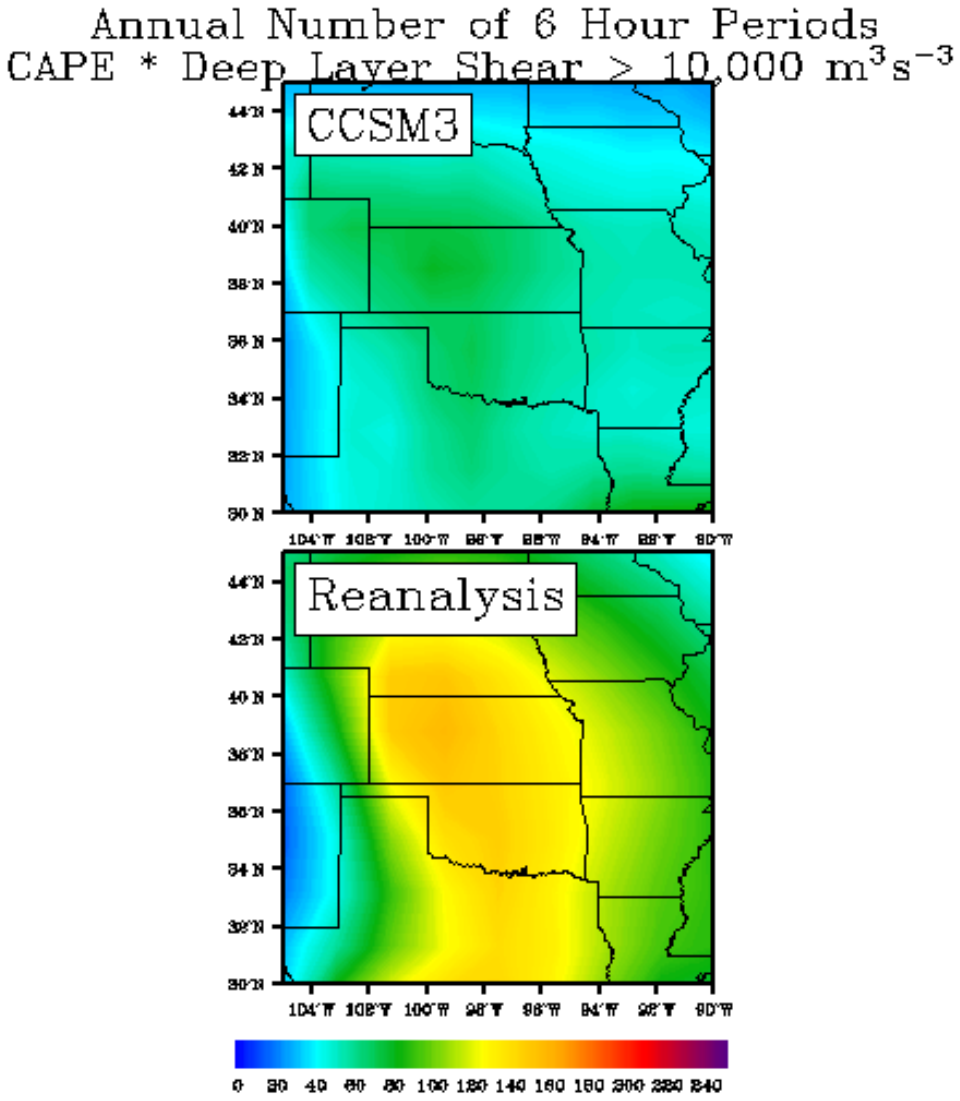


Fig 4.6: Annual number of 6 hour periods with environments favorable for severe convective weather. The CCSM (left) is averaged over 20 years while the reanalysis (right) is averaged over 42 years.

interesting, but not surprising, to note that the absolute maximum located over the Gulf Stream consists of double the values of the relative maximum in the central plains. Neglecting the Gulf Stream bias, the spatial distributions in Figure 4.5 are qualitatively similar as well. A maximum occurs on the lee side of the Rocky Mountains in the central plains with decreasing occurrence further east. One difference is the northern extent of the CCSM3 product is significantly less than that of the reanalysis. Even with this difference, it is significant to note that the spatial distribution of the CCSM3 product of deep layer shear and CAPE is consistent with that of observed maximum in occurrence of severe weather in North America (Rasmussen and Blanchard, 1998).

Once again, the spatial distribution appears to favor regions of warm water. Focusing solely on the central United States (Figure 4.6) greatly reduces the number of regions experiencing this bias. It is readily seen that the spatial distributions qualitatively agree. Furthermore, qualitatively the reanalysis frequency is once again slightly double that of the CCSM3.

Figure 4.7 shows the diurnal cycle of CAPE for the central United States computed for both the CCSM3 and the reanalysis. In both the CCSM3 and the reanalysis the mean CAPE for 00Z is the greatest for all months, followed by 18Z, 06Z, and lastly 12Z. This makes physical sense as on average the highest CAPE values would be expected in the late afternoon which corresponds to 00Z in the central plains of the United States. On average the lowest CAPE would be expected in the morning which corresponds to 12Z.

The CCSM3 diurnal cycle of mean CAPE peaks in June and then begins a fairly steady decline. The reanalysis also peaks in June with the exception of the 18Z time which peaks in July, however the reanalysis does not begin to decline until after July. Also, of particular interest is the quantitative similarity between the CCSM3 and reanalysis at 00Z. This quantitative similarity is not seen in any of the other times, especially in the warm seasons, as the CCSM3 mean CAPE values at the other times are less than half as large as the reanalysis values.

The CCSM3 also exhibits interannual variability similar to that observed. Figures 12 and 13 show spatial distributions of the product of CAPE and deep layer shear greater than 10,000 $m^3 s^{-3}$ for a handful of years. Note that these are intended to show the typical interannual changes in the simulated frequency of severe weather environments and should not be compared to the same years in the reanalyses. However, it is reasonable to compare the simulated interannual variability to the typical observed year-to-year variations in occurrence of severe weather. Simulated model year 1981 indicated a relative maximum in occurrence in northeast Colorado, while in simulated model year 1986 the relative maximum was located in the southeast United States. Simulated model year 1990 had a relative maximum over the southern plains and the Gulf of Mexico while simulated year 1991 had a relative minimum over the Gulf of Mexico. Simulated year 1995 had a relative maximum over the mid-Atlantic and Ohio Valley region. Simulated year 1996 had a relative minimum over the entire United States, while simulated year 1999 had a relative maximum over the same region.

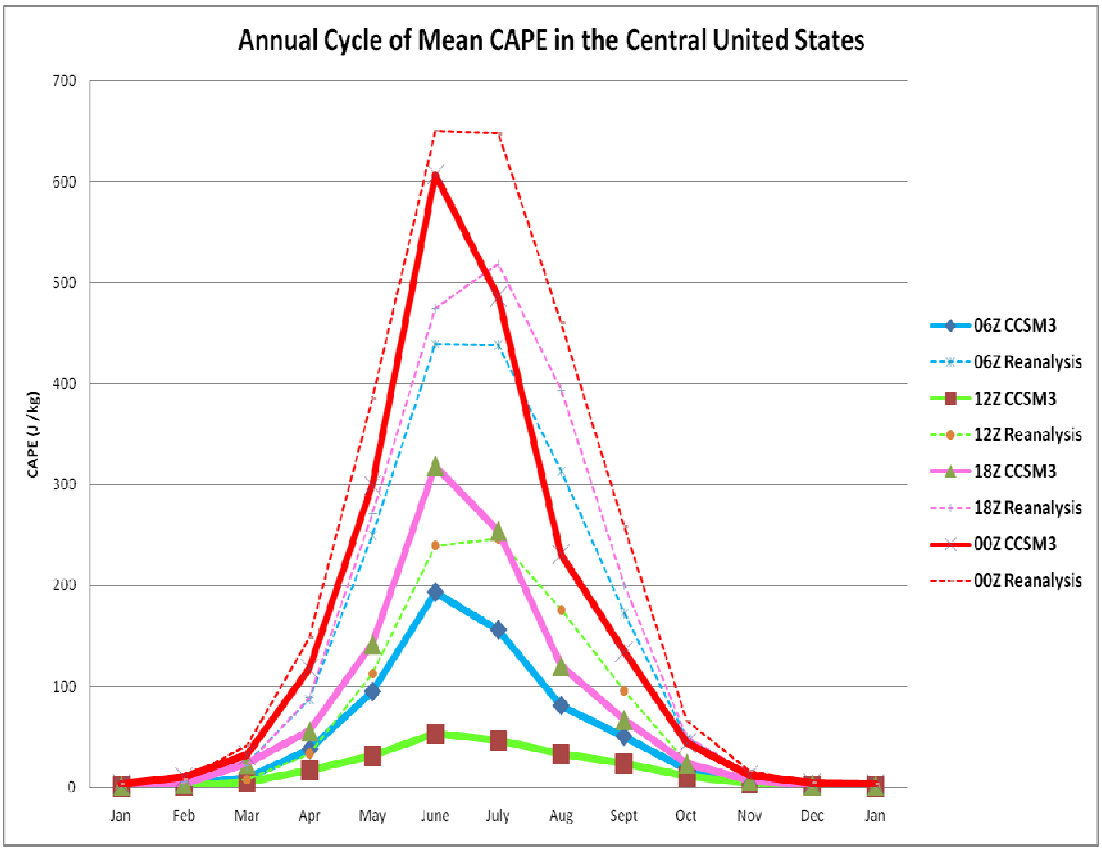


Fig. 4.7: Annual Cycle of Mean CAPE in the Central United States. Solid lines represent CCSM3 and dashed lines represent Reanalysis.

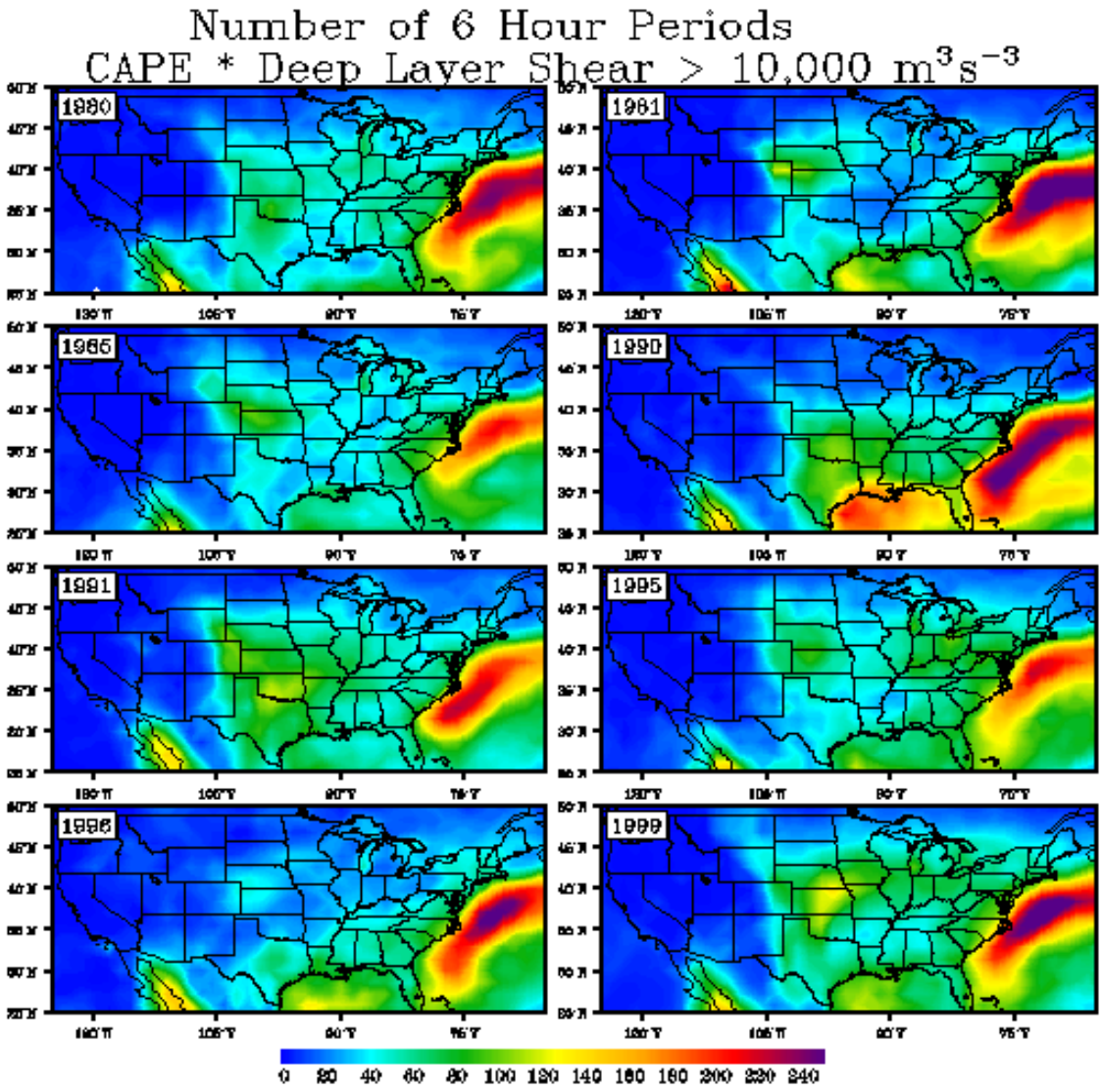


Fig 4.8: Interannual Variability of the CCSM3. The color scale is the same as that in Figure 4.5.

4.2 Discussion

The CCSM3 has shown a great deal of promise in resolving the spatial distributions of severe weather environments, as proxied by CAPE and the product of CAPE and deep layer shear. In areas well removed from warm water, the CCSM3 observed values of mean CAPE are quantitatively about half the magnitude of the reanalysis as shown in Figure 10. The spatial distribution of mean CAPE is consistent with that of the reanalysis data and observations. A relative maximum of mean CAPE is found collocated with the relative maximum of the reanalysis. A comparison of the frequency distributions over the central United States between the CCSM3 and reanalysis reveals a similar structure.

While over the central United States the CCSM3 produces physically intuitive results, the same cannot be said over the entire North American domain. Regions over the Gulf of Mexico, Gulf of California, Gulf Stream Current, and even Lake Michigan have relative maximums that are not found in the reanalysis. The higher probability of the CCSM3 in producing CAPE values over areas of warm water should not detract from the CCSM3s ability to qualitatively recreate the mean seasonal CAPE field over the central United States.

Additionally, the CCSM3 shows a strong signal that interannual variations of the spatial distributions are similar to those variations observed naturally. The CCSM3 has both active, or hot, years (frequent high CAPE times deep layer shear in similar locations) as well as inactive, or cold, years. Furthermore the spatial location of the relative maxima varies from year to year between the central and high plains of

the United States to the southern plains to the southeast to the Ohio Valley - consistent with observations.

Chapter 5: Future Climate Simulations

Few, if any, studies have attempted to examine severe weather environments (for example high values of the product of CAPE and deep layer shear) under climate change; however a couple of studies have examined CAPE under climate change. Results from Ye et al. (1998) indicate that climate sensitivity of CAPE to surface temperature in the Goddard Institute for Space Studies GCM is around an order of magnitude less than observed sensitivities. The resolution of this model is 4º by 5º which is may be too coarse to adequately resolve significant increases in CAPE. Additionally, the aforementioned study only examined CAPE in the tropics. Niall and Walsh (2005) used the CSIRO Mk3 GCM to examine CAPE under a doubling of CO2 from pre-industrial levels in Australia. Their results indicate that CAPE significantly decreases in the future, perhaps due to drying in this region in the simulated future climate. However, while the CSIRO Mk3 GCM has a better resolution (approximately 1.875º by 1.875º), only two locations were examined and cannot be taken as representative of the entire mid-latitudes.

The consistent quantitative shortcomings in current climate models in trying to represent the current climate of CAPE does not necessarily stand as a hindrance to making estimates about severe weather environments in the future. These shortcomings simply prevent scientists from taking $dCAPE/d\varphi$ for the current climate (where φ represents any atmospheric variable), multiplying it by the climate change in φ, and expect to find the climate change in CAPE. This is due to the different way the atmosphere responds to unforced synoptic variability versus radiatively forced near-equilibrium climate change (Del Genio, personal communication). Thus all one

can do is to demonstrate that a given model is reasonable in simulating the current climate and then let it make its prediction for the change climate - taking into account the simulated change in atmospheric structure due to radiative forcing (Ye et al., 2003 ; Del Genio, personal communication). It was just shown that the CCSM3 produces physically intuitive severe weather environments over land under the present climate. Thus it is reasonable to examine the CCMS3's simulations of severe weather environments under climate change conditions.

5.1 Results from CCSM3 SRES A2 21st Century Simulation

The seasonal cycle of mean CAPE values in the CCSM3 A2 scenario for the period 2080-2099 (hereafter simply referred to as the future scenario) is presented in Figure 5.1. In the winter months mean CAPE values greater than 50 J kg^{-1} are restricted to areas over warm water or near regions of warm water (e.g., the Florida peninsula). In spring, the mean CAPE values increase across the eastern two-thirds of the United States south of 40ºN with highest values located across the western Gulf of Mexico and eastern Texas, northward into southern Oklahoma. Investigating the summer mean CAPE values, increases everywhere but the western United States are found as compared to the spring mean CAPE values. A relative maximum over the northern plains is found during the summer along with absolute maxima over the Gulf Stream and the western Gulf of Mexico. Interestingly, a relative minimum in mean CAPE exists over southeast Oklahoma, northeast Texas, and western Arkansas. By autumn the largest mean CAPE values are confined to the Gulf of California, western Gulf of Mexico, and the southern Gulf Stream. Interestingly, mean CAPE values of

between 50 and 150 J kg^{-1} still remain over much of the eastern two-thirds of the United States.

A comparison of the seasonal cycle of mean CAPE from the CCSM3 20^{th} century simulation (hereafter referred to as the current scenario) to the future scenario demonstrates qualitatively similar results. Both seasonal cycles place seasonal maximums (relative and absolute) in similar locations. The numerical values of mean CAPE have increased in most if not all locations in all seasons in the future scenario with a possible exception being the summer relative minimum located over southeast Oklahoma, northeast Texas, and western Arkansas. Higher mean CAPE values appear to last longer into the year in the future scenario compared to the current scenario as evident by the larger area and more northward extent of mean CAPE values greater than 100 J kg^{-1} in autumn.

Comparison of the seasonal cycle of mean deep layer shear from the current to future scenario (Figure 5.2) indicates a seemingly physical evolution between seasons. The highest mean deep layer shear values in both scenarios are found in the winter across the north and decrease toward the south. In the spring and summer, the mean values decrease everywhere and then begin to increase once again in autumn.

After using the normalization process discussed previously, a frequency distribution in log – CAPE space was created comparing the frequency of CAPE in the future scenario to the current scenario (Figure 5.3) over the North American domain. Both distributions are fairly similar in structure - bimodal with the first peak between $10^{1.6}$ and $10^{1.8}$ (~ 40 and 60) J kg^{-1} and a primary peak around 10^{3} (~ 1000) J kg^{-1}. The distributions are nearly identical up through CAPE values of $10^{2.8}$ (~ 630) J

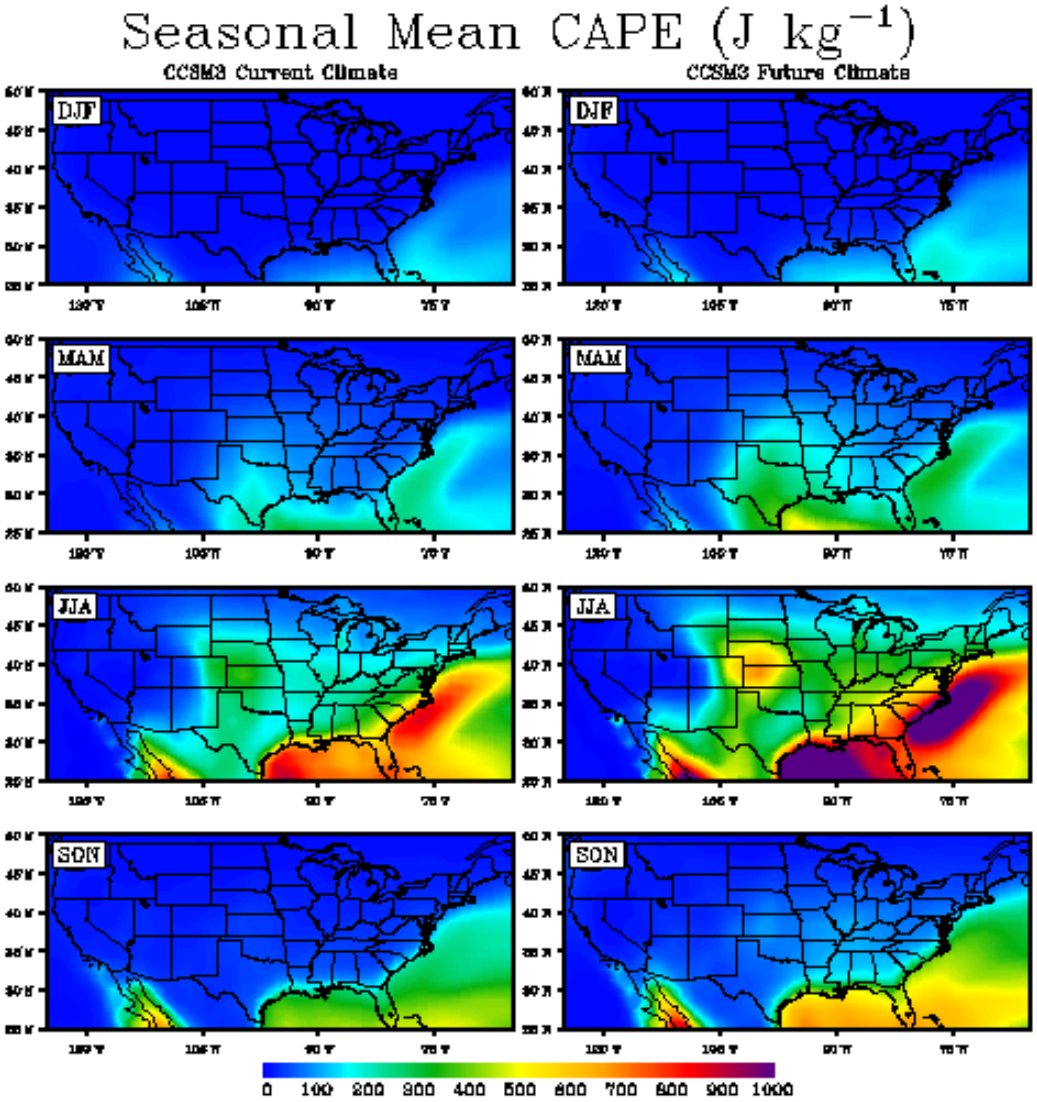


Fig5.1: Mean CAPE values by season for both the current simulation (left column) and the future simulation (right column). Note that both sets of output are averaged over 20 years.

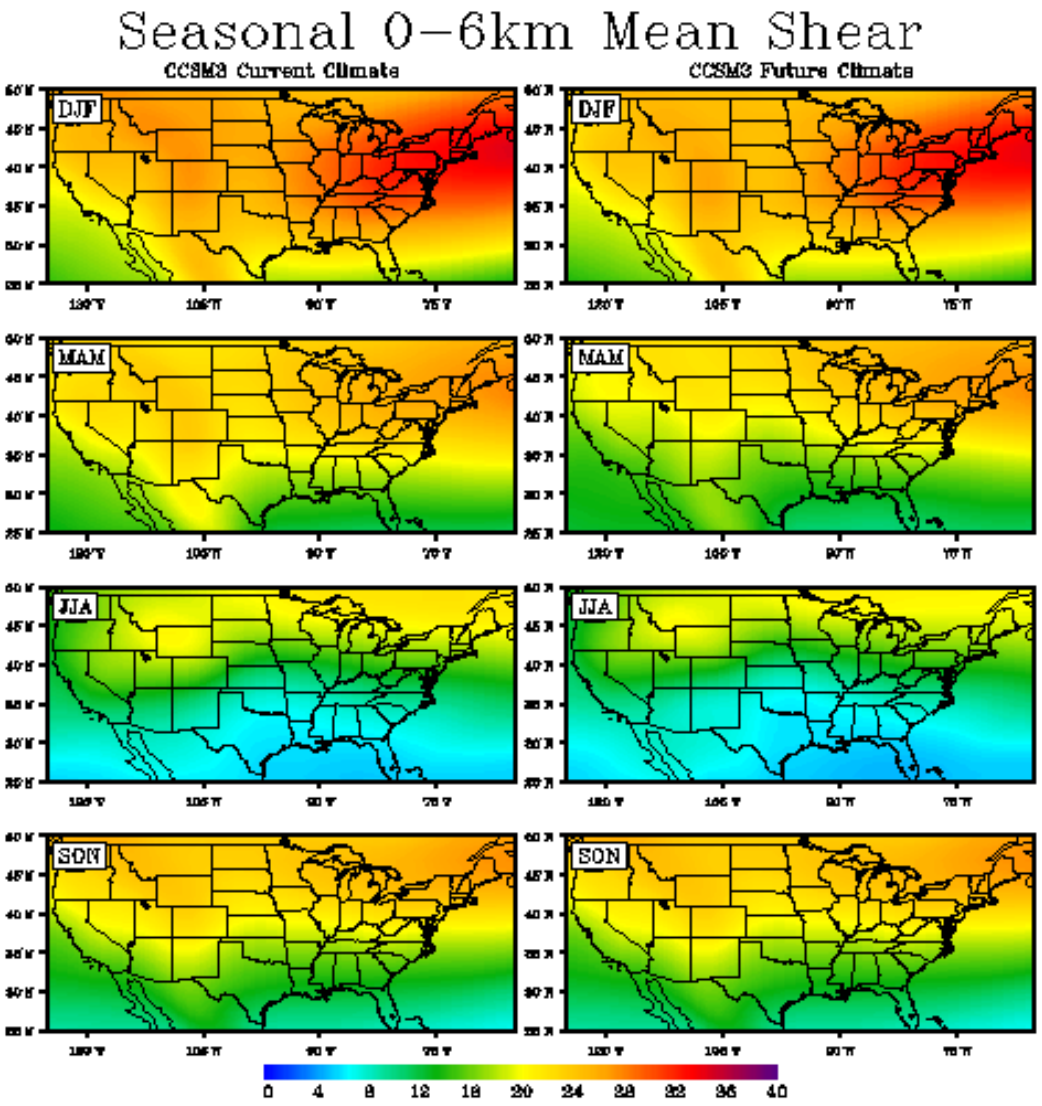


Fig5.2: Mean 0-6 km shear values by season for both the future simulation (left) and the current simulation (right). Both sets of output are averaged over 20 years.

kg^{-1}, with the future scenario being equal or slightly greater than the current scenario. For CAPE values greater than $10^{2.8}$ (~ 630) J kg^{-1} the future scenario results in a much higher frequency of CAPE with the exception of CAPE values greater than approximately 4000 J kg^{-1} when both distributions are once again about equal.

After using the normalization process discussed previously, a frequency distribution in log – CAPE space was created comparing the frequency of CAPE in the future scenario to the current scenario (Figure 5.3) over the North American domain. Both distributions are fairly similar in structure - bimodal with the first peak between $10^{1.6}$ and $10^{1.8}$ (~ 40 and 60) J kg^{-1} and a primary peak around 10^3 (~ 1000) J kg^{-1}. The distributions are nearly identical up through CAPE values of $10^{2.8}$ (~ 630) J kg^{-1}, with the future scenario being equal or slightly greater than the current scenario. For CAPE values greater than $10^{2.8}$ (~ 630) J kg^{-1} the future scenario results in a much higher frequency of CAPE with the exception of CAPE values greater than approximately 4000 J kg^{-1} when both distributions are once again about equal.

Once again, in an effort to remove any possible bias introduced by warm water, a normalized frequency distribution for the central plains was also examined in log – CAPE space. The shape of this normalized frequency distribution for the future scenario is similar to that of the current scenario; although, the frequency of occurrence increases more for the higher CAPE environments. Furthermore, the maximum frequency of occurrence (in log – CAPE space) has increased from $10^{2.8}$ to 10^3 (~ 630 to 1000) J kg^{-1} in the current scenario to 10^3 to $10^{3.2}$ (~1000 to 1600) J kg^{-1} to in the future scenario.

A CAPE – deep layer shear normalized joint distribution plot for the future scenario over the central United States showing the annual frequency of CAPE and deep layer shear values and is shown in Figure 5.5. This distribution exhibits a similar structure as the CAPE distribution – a small region of relatively low CAPE and high shear and a larger region of high CAPE and lower shear. The CAPE – deep layer

shear normalized joint distribution plots for both the current scenario (Figure 5.5) and future scenario exhibit an absolute maximum in the region with high CAPE and lower shear, albeit the future scenario appears to be more than the current scenario.

The spatial distribution of the annual number of 6-hourly periods with the product of CAPE and deep layer shear greater than 10,000 $m^3 s^{-3}$ in Figure 5.6 reveals a relative maximum located over the central plains of the United States. It is interesting, but not surprising, to note that the absolute maximums located over the Gulf Stream and Gulf of Mexico still consists of double the values of the relative maximum in the central plains. Comparing the future scenario to the current scenario, the spatial distributions in Figure 5.6 are qualitatively similar as well. A maximum occurs on the lee side of the Rocky Mountains in the central plains with decreasing occurrence further east. The main difference is found when comparing the quantitatively values of the mean CAPE which are substantially higher in the future scenario.

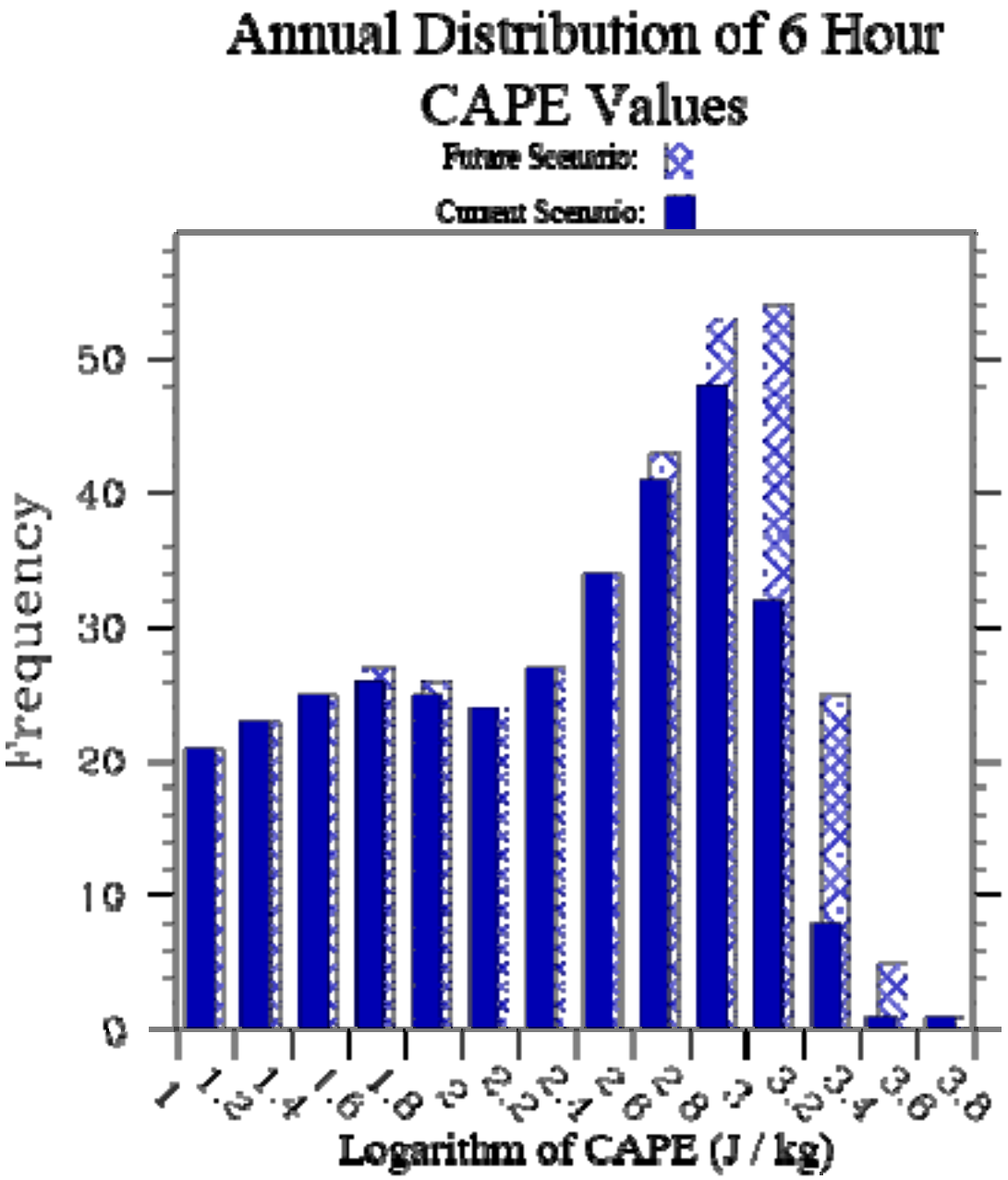


Fig 5.3: Annual Distribution of 6 Hour CAPE Values over the entire North American domain. The future scenario is checkered while the current scenario is solid.

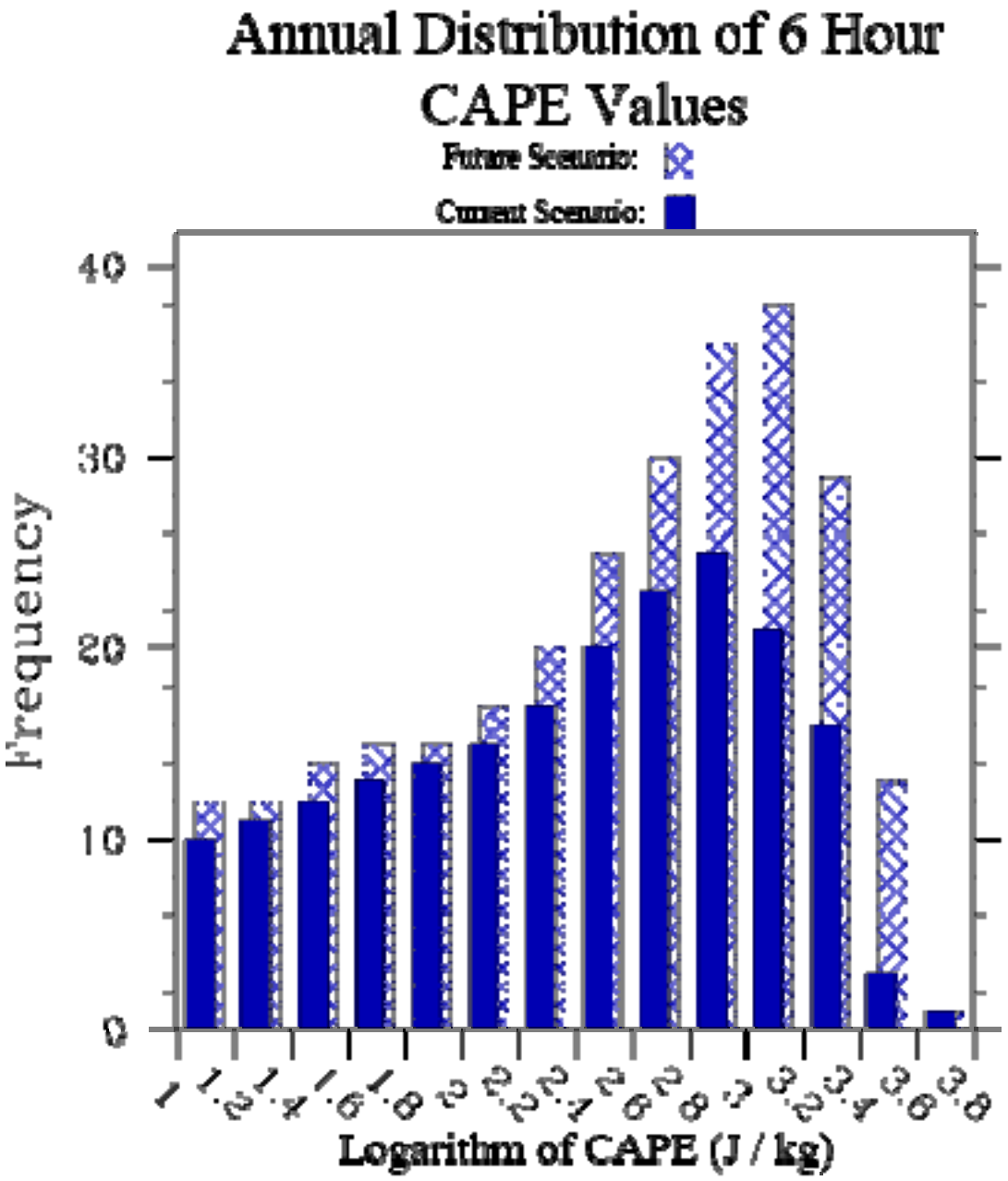


Fig 5.4: Annual Distribution of 6 Hour CAPE Values over the central United States domain. The future scenario is checkered while the current scenario is solid.

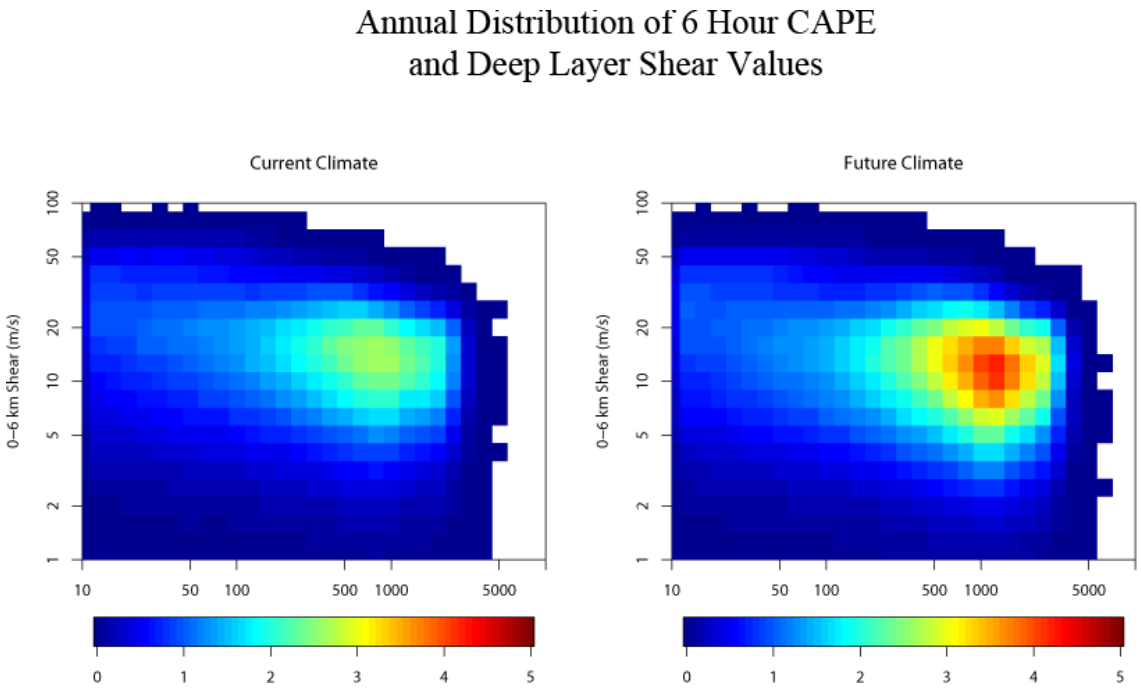


Fig 5.5: Normalized joint distribution plot of CAPE and deep layer shear for the central United States. The current scenario is on the left and the future scenario is on the right.

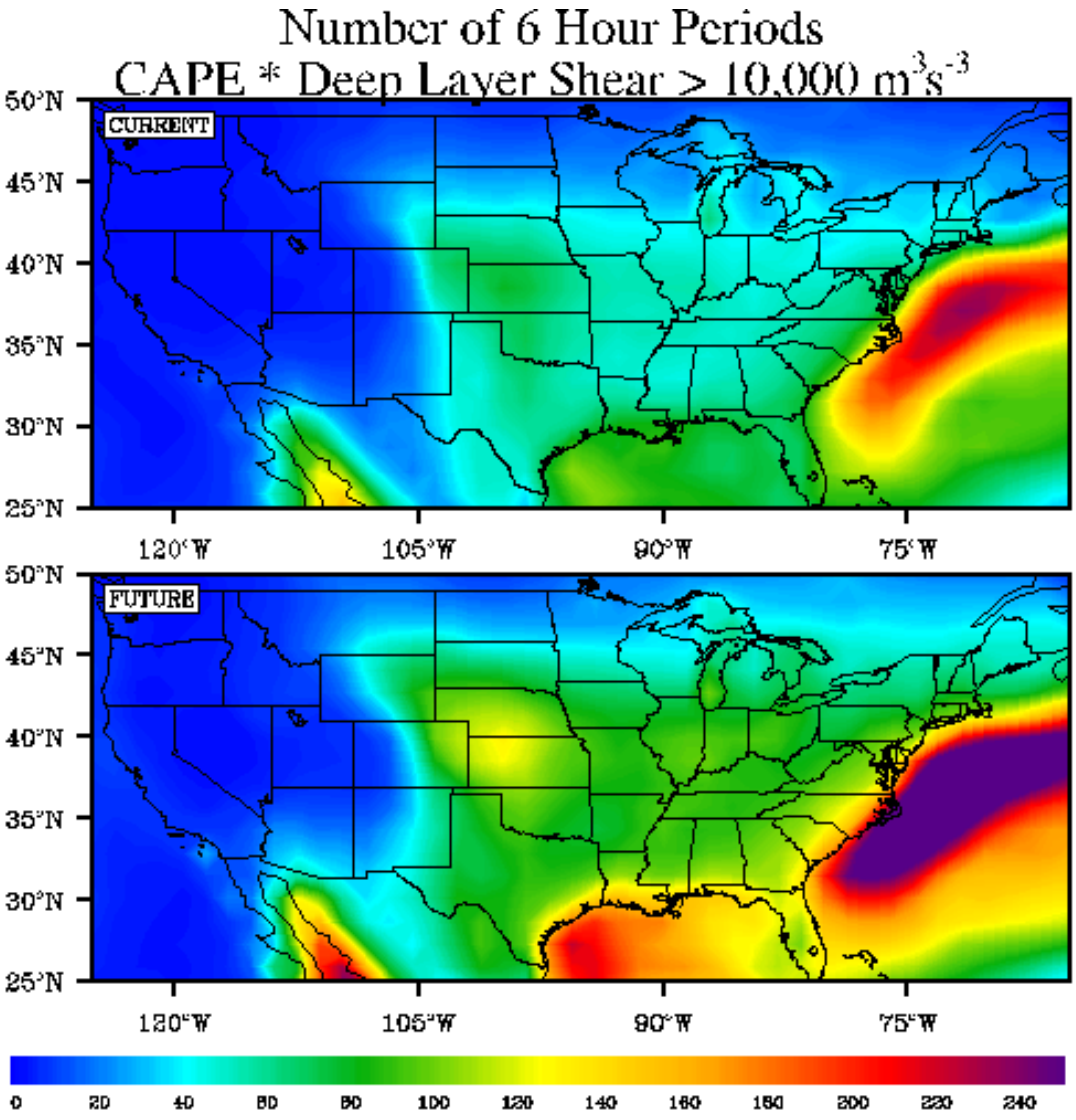


Fig 5.6: Annual number of 6 hour periods with environments favorable for severe convective weather. The current scenario (top) and the future scenario (bottom) is averaged over 20 years.

Focusing solely on the central United States (Figure 5.7) greatly reduces the number of regions experiencing the previously mentioned bias over warm water. It is readily seen that the spatial distributions are qualitatively similar between the future scenario and the current scenario with the caveat that the future scenario's frequency is once again higher than that of the current scenario.

Figure 5.8 shows the diurnal cycle of CAPE for the central United States computed for both the future and current scenarios. The seasonal and diurnal cycle of mean CAPE is surprisingly similar between the future and current scenarios with maximums all occurring in June and with similar the same monthly increase up to the maximum and decrease after the maximum. The primary difference between the two scenarios is that the future scenario's mean CAPE is larger every month than the current scenario.

The future scenario also captures a realistic interannual variability. Figure 5.9 shows simulated model years of the product of CAPE and deep layer shear greater than 10,000 $m^3 s^{-3}$ for the future scenario. Some model years the Gulf of Mexico is in a relative minimum (2086) while others it is still active. Some model years have the southern plains of the United States very active (2096) while other years the southern plains are inactive (2086 and 2089). The same can be said of other regions as well.

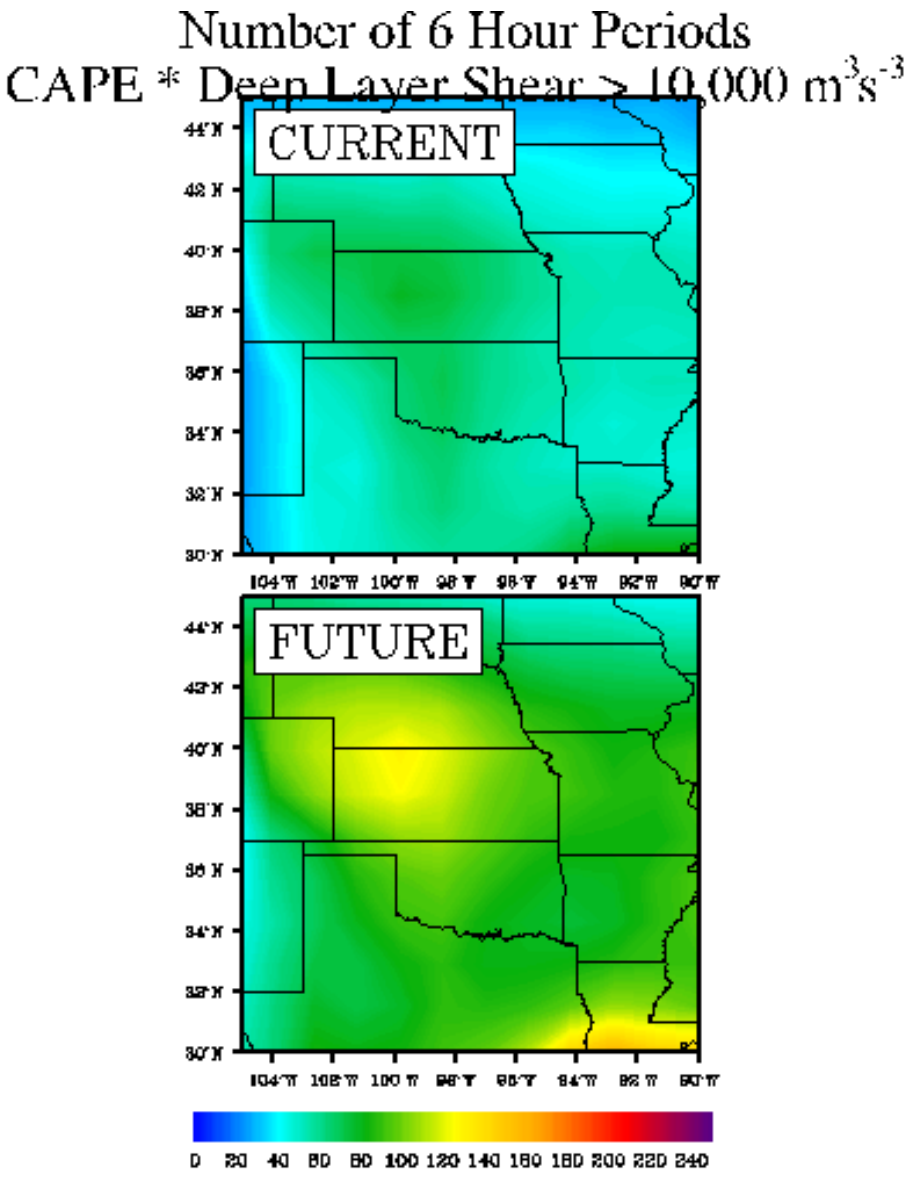


Fig 5.7: Annual number of 6 hour periods with environments favorable for severe convective weather over the central United States. The current scenario (top) and the future scenario (bottom) is averaged over 20 years.

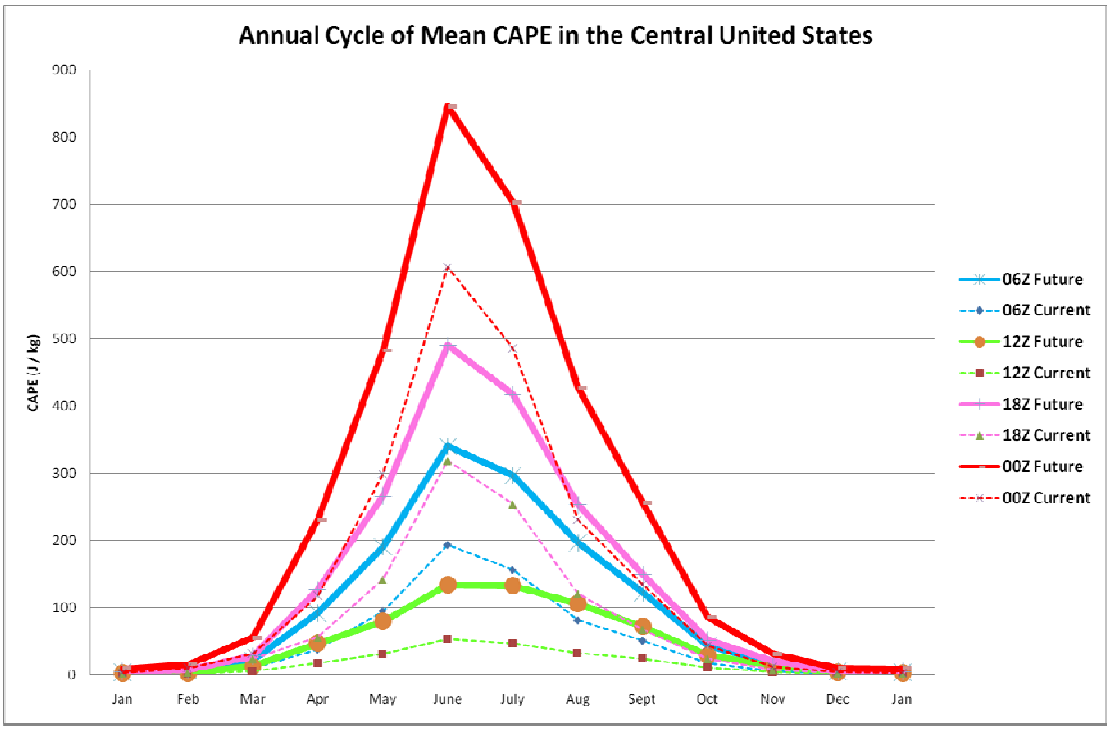


Fig. 5.8: Annual Cycle of Mean CAPE in the Central United States. Solid lines represent CCSM3 and dashed lines represent Reanalysis.

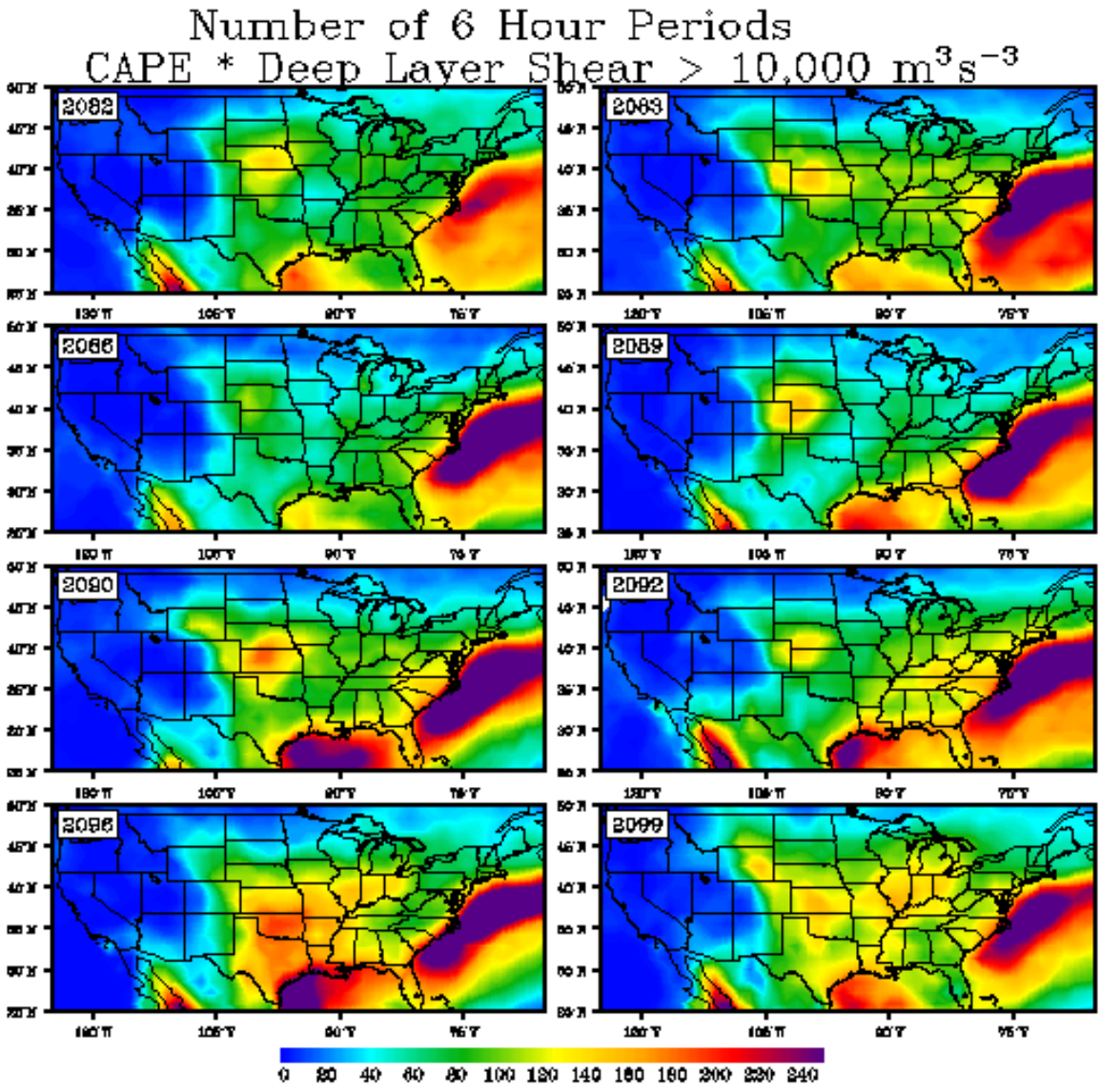


Fig 5.9: Interannual Variability of the CCSM3. The color scale is the same as that in Figure 5.6

5.2 Discussion

The future scenario indicates an increase in the number of 6 hour periods with environments conducive for the development of severe convective weather. While the regions experiencing warm water biases show fairly substantial increases in mean CAPE, other regions experience increases as well. A quick comparison of the mean CAPE from the future scenario to the current scenario shows that CAPE does not decrease anywhere east of the Rocky Mountains. The only place that shows a decrease in mean CAPE extends from central California out over the Pacific Ocean. In the eastern United States the largest increase in CAPE is found over the northwestern Gulf of Mexico with additional large increases found over the Gulf Stream Current, Gulf of California, and northwest Kansas. Comparing the increase of mean CAPE in terms of percent increase from the current simulation shows that nearly everywhere east of the Mississippi River has an increase of over 100% in mean CAPE with the region near Lake Michigan receiving the highest percentage increases (over 200%).

Examining the increase of mean CAPE for each season indicates that the greatest increase in mean CAPE is found in summer over northwest Kansas – southwest Nebraska and from the northwestern Gulf of Mexico over to the Gulf Stream Current. One of the smallest increases in mean CAPE occurs over north-central Texas and extends into western Arkansas during the summer. In this region mean CAPE values have increase by less than 100 J kg^{-1} compared to the increase of over 150 J kg^{-1} in the surrounding areas. In terms of the actual increase of mean CAPE, winter has an increase of less than 25 J kg^{-1} everywhere except for regions

over warm water. In terms of percentages, winter has the greatest increase of mean CAPE than any other month, especially along the United States – Canadian border east of the Rockies (greater than 300%). Autumn has an increase of around 50 to 100 J kg^{-1} of mean CAPE across the southeast United States into the Midwest. In terms of percents, this is nearly a 300% increase in some places when compared to the current scenario.

A close inspection of the seasonal cycle of mean CAPE clearly shows the greatest decrease in mean CAPE occurs over the central and southern portions of the United States. The most noticeable change in the future occurs in spring when the shear contours have the greatest push northward. Examining the mean CAPE for the entire year shows that the greatest decrease in mean CAPE occurs over the southwestern United States which is still only 2 m s^{-1}.

Examining the difference in the CAPE – deep layer shear distribution between the future and current scenarios indicates that almost nowhere does the frequency of occurrence decrease. The greatest increase is found in the high CAPE, moderate deep layer shear. It should be pointed out that the greatest increases of occurrence are in regions where the product of CAPE and deep layer shear is greater than 10,000 m^3 s^{-3}. This indicates that the most substantial increase occurs in environments conducive for the development of severe convective weather.

The spatial distributions of the annual number of 6 hour periods with the product of CAPE and deep layer shear greater than 10,000 m^3 s^{-3} has not changed all the much between the future and current scenarios. Relative and absolute maximums are still generally collocated between the two scenarios. The main difference is the

increase in the number of periods in the future scenario. As for the seasonal and diurnal cycle, a similar pattern exists in both the future and current scenarios with mean CAPE values having increased at all times for all months.

Chapter 6: Discussion

The CCSM3 has shown great deal of promise in resolving the spatial distributions of severe weather environments. While the CCSM3 computes values are qualitatively about half the magnitude of the reanalysis values, as shown in Figure 4.4, , the spatial patterns of estimated severe weather environments (Figure 4.5) make intuitive sense. Relative maxima in the distributions of CAPE and CAPE multiplied by deep layer shear are found in the central United States collocated with the relative maxima in the reanalysis data.

Examination of the CCSM3's seasonal cycle of mean CAPE once again captures the same qualitative patterns of the reanalysis data. The CCSM3 reveals a similar diurnal cycle to that of the reanalysis with 00Z doing the best. Looking at the product of CAPE and deep layer shear shows similar results as the examination of mean CAPE, namely, that the spatial distributions are qualitatively similar with the numerical values being less by a factor of a little less than two. The exception to both the mean CAPE and the product of CAPE and deep layer shear is found over areas with warm water (e.g., Gulf of Mexico and Gulf Stream Current) where the CCSM3 is considerably higher than that of the reanalysis.

Additionally, the CCSM3 shows a strong signal that interannual variations of the spatial distributions are similar to those variations observed naturally. The CCSM3 has both active years (frequent high CAPE times deep layer shear in similar locations) as well as inactive years. Furthermore, the spatial location of the relative maxima varies from year to year between the central and high plains of

the United States to the southern plains to the southeast – consistent with observations.

Using the A2 SRES emissions scenario, the CCSM3 indicates an increase in mean CAPE over current values everywhere east of the Rocky Mountains by 2099. The same can be true of the annual number of 6 hour periods of the product of CAPE and deep layer shear. While the annual number of periods of the product of CAPE and deep layer shear increase almost everywhere, in the summer months it appears that little if any change is found in north central Texas.

In an effort to assess the significance of the increase in severe weather environments a Student's T Test was used on the entire North American domain as well as on sub-domains of various sizes within the North American domain. In every domain used the resulting probability that the future mean came from the same population as the current mean was less than 10^{-10}%. Similar values were found when assessing the increase in mean CAPE. Thus it can be said the increase in mean CAPE and in the annual number of 6 hour periods with the product of CAPE and deep layer shear greater than 10,000 m^3 s^{-3} in the future scenario is significant.

Both the current and future simulations appear to capture a realistic interannual variability. Most regions in the future have years with fewer occurrence of environments conducive to severe weather than in the current – even though the mean values for the United States is always higher in the future simulation than the current simulation. The same holds true for the values of mean CAPE. Thus, even though the means for the entire North American domain have increased, there still exists a large variability from year to year at any one location.

Examining both mean CAPE values and mean deep layer shear values separately sheds light on what appears to be the driving force behind the increase in severe weather environments. Mean deep layer shear values have decreased over most of the United States, but less than 2 m s^{-1}, while at the same time mean CAPE values have increased by over 50 J kg^{-1} with local amounts increasing by over 200 J kg^{-1}. Therefore, even though deep layer shear does decrease, CAPE increases by more than enough to compensate.

The most plausible reason for the deficiencies in mean CAPE and in the annual number of severe convective weather environments in the CCSM3 over the central United States (as compared to the reanalysis) has to do with the convective scheme of the CCSM3. The CCSM3 uses a Zhang – McFarlane convective scheme for deep convection, which effectively produces convection anytime there is enough CAPE to overcome the stable layer. Examination at the convective inhibition (CINH; defined to be the accumulated negative buoyancy for the parcel), it is found that there is no CINH unless CAPE is greater than 100 J kg^{-1}; CAPE greater than 100 J kg^{-1} never exists unless CINH is present. Additionally, examination of CAPE animations for both the 20 years in the current scenario of the 20 years of the future scenario indicates that CAPE tends to be generated in the presence of synoptic scale systems There is little signal that the CCSM3 generates the almost daily 1000 J kg^{-1} of CAPE that observations and reanalysis tend to produce over the central plains during the warm season. This lack of almost daily CAPE could have a significant impact in mean CAPE calculations.

The high mean CAPE bias found over regions of warm water appears to be related to a coupling problem between the ocean and atmosphere models. It is hypothesized that the coupler allows too large of a heat and moisture flux into atmospheric model. This increased influx of low-level heat and moisture allows for generation of larger CAPE. Investigations show that while the largest CAPE values are generated over the plains of the United States, the relative rare occurrence of the higher CAPE values leads to lower mean values. This contrasts to the almost daily occurrence of moderate CAPE values over regions of warm water, which in turn produce a higher mean.

While the results of this study indicate a dramatic increase in severe weather environments in the future, the results must be taken in context. This study only uses one model. This one model has coarse resolution in both the horizontal and vertical. Additional caveats of the model include the use of only one convective scheme and the inability to resolve clouds, subsidence, capping inversions, and other mesoscale features important to the development of CAPE and thunderstorm initiation. Thus there is a need to evaluate other global climate models in an effort to further assess the climate sensitivity to global climate models' parameterized processes. Future work will also focus on the use of regional models nested within global climate models in an attempt to make use of the regional models' higher resolution and convective schemes. Lastly, this study focused on only one emission scenario. A need still exists to examine other emission scenarios as well.

References

Brooks, H. E., and C. A. Doswell, III, 2001: Normalized damage from major tornadoes in the United States: 1890–1999. Wea. Forecasting, 16, 168-176.

_____, J. W. Lee, and J. P. Craven, 2003: The spatial distribution of severe thunderstorm and tornado environments from global reanalysis data. Atmos. Res., 6768, 73-94.

_____, A. R. Anderson, et al., 2007: Climatological aspects of convective parameters from the NCAR/NCEP reanalysis. Atmos. Res., 83, 294-305.

Brown, B.G., A. H. Murphy, 1996: Verification of aircraft icing forecasts: the use of standard measures and meteorological covariates. Preprints, 13th Conf. Probability and Statistics in the Atmospheric Sciences, San Francisco, California, USA, Amer. Meteorol. Soc., pp. 251-252

Cubasch, U., et al., 2001: Projections of Future Climate Change. In: IPCC, 2001: *Climate Change 2001: The Scientific Basis.* Contributions of Working Group I to the Third Assessment Report of the Intergovernmental Panel on Climate Change [Houghton, J.T., et al.]. Cambridge University Press, Cambridge, United Kingdom and New York, NY, USA, 881pp.

Collins W. D., et al., 2004: Description of the NCAR Community Atmosphere Model (CAM 3.0). NCAR Technical Note, NCAR/TN-464+STR, 2004

_____, et al., 2006: The Community Climate System Model version 3 (CCSM3). J. Climate, 19, 2122–2143

Doswell, C. A. III, Brooks, H. E., and Kay, M. P., 2005: Climatological estimates of daily local nontornadic severe thunderstorm probability for the United States. Wea. and Forecasting, 20, 577-595

IPCC, 2001: *Climate Change 2001: The Scientific Basis.* Contributions of Working Group I to the Third Assessment Report of the Intergovernmental Panel on Climate Change [Houghton, J.T., et al.]. Cambridge University Press, Cambridge, United Kingdom and New York, NY, USA, 881pp.

Kalnay, E., et al., 1996. The NCEP/NCAR 40-year reanalysis project. Bull. Am. Meteorol. Soc. 77, 437–472.

Lee, J.W., 2002. Tornado proximity soundings from the NCEP/NCAR reanalysis data. MS Thesis, University of Oklahoma. 61 pp.

Nakicenovic, N., et al., 2000: *Special Report on Emission Scenarios.* IPCC, Cambridge University Press, Cambridge, United Kingdom and New York, NY, USA, 570pp.

Niall, S., and K. Walsh, 2005: The impact of climate change on hailstorms in southeastern Australia. Int. J. Climatol. 25: 1933–1952.

National Weather Service (NWS), 1997: Summary of U.S. natural hazard Statistics for 1997. Office of Climate, Water, and Weather Services, 1998

_____, 1998: Summary of U.S. natural hazard Statistics for 1998. Office of Climate, Water, and Weather Services, 1999

_____, 1999: Summary of U.S. natural hazard Statistics for 1999. Office of Climate, Water, and Weather Services, 2000

_____, 2000: Summary of U.S. natural hazard Statistics for 2000. Office of Climate, Water, and Weather Services, 2001

_____, 2001: Summary of U.S. natural hazard Statistics for 2001. Office of Climate, Water, and Weather Services, 2002

_____, 2002: Summary of U.S. natural hazard Statistics for 2002. Office of Climate, Water, and Weather Services, 2003

_____, 2003: Summary of U.S. natural hazard Statistics for 2003. Office of Climate, Water, and Weather Services, 2004

_____, 2004: Summary of U.S. natural hazard Statistics for 2004. Office of Climate, Water, and Weather Services, 2005

_____, 2005: Summary of U.S. natural hazard Statistics for 2005. Office of Climate, Water, and Weather Services, 2006

_____, 2006: Summary of U.S. natural hazard Statistics for 2006. Office of Climate, Water, and Weather Services, 2007

Oleson, et al., 2004: Technical Description of the Community Land Model (CLM 3.0). NCAR Technical Note, NCAR/TN-461+STR, 2004

Rasmussen, E.N. and D.O. Blanchard, 1998: A baseline climatology of sounding-derived supercell and tornado forecast parameters. Weather Forecast. 13, 1148-1164

Ye, .B., A. D. Del Genio, and K. K.-W Lo, 1998: CAPE variations in the current climate and in a climate change. J. Climate, 11, 1997-2015.

Vertenstein, M. et al., 2004: CCSM3.0 User's Guide. NCAR, 2004

Zhang, G. J., and N. A. McFarlane, 1995: Sensitivity of climate simulations to the parameterization of cumulus convection in the Canadian Climate Centre general circulation model. Atmosphere-Ocean. 33, 407-446, 1995